

AperTO - Archivio Istituzionale Open Access dell'Università di Torino

**Air pollution deposition on a roadside vegetation barrier in a Mediterranean environment:
Combined effect of evergreen shrub species and planting density**

This is the author's manuscript

Original Citation:

Availability:

This version is available <http://hdl.handle.net/2318/1691102> since 2020-07-08T11:49:40Z

Published version:

DOI:10.1016/j.scitotenv.2018.06.217

Terms of use:

Open Access

Anyone can freely access the full text of works made available as "Open Access". Works made available under a Creative Commons license can be used according to the terms and conditions of said license. Use of all other works requires consent of the right holder (author or publisher) if not exempted from copyright protection by the applicable law.

(Article begins on next page)

1 **J. Mori^{a*}, A. Fini^b, M. Galimberti^b, M. Ginepro^c, G. Burchi^d, D. Massa^{d#}, F. Ferrini^{a#}**

2 ^a *Department of Agrifood Production and Environmental Sciences, section Woody Plants -*

3 *University of Florence, Italy*

4 ^b *Department of Agricultural and Environmental Sciences – Production, Landscape, Agroenergy –*

5 *University of Milan, Milan, Italy*

6 ^c *Department of Chemistry – University of Turin, Italy*

7 ^d*CREA Research Centre for Vegetable and Ornamental Crops, Council for Agricultural Research*

8 *and Economics, Piacenza, Italy*

9 *corresponding author: email: jacopo.mori@unifi.it, Viale delle Idee 30, 50019 Sesto Fiorentino

10 (FI), phone: +390554574059

11 # These authors contributed equally to this work

12

13 **Title:** Air pollution deposition on a roadside vegetation barrier in a Mediterranean

14 environment: combined effect of evergreen shrub species and planting density

15

16 **Highlights**

- 17 • Higher LAI induced higher deposition, while planting density was not a determinant
- 18 • Vegetation barrier changed deposition dynamics in the experimental site
- 19 • Image analysis differentiated between on-leaf PM with different colorations
- 20 • On-leaf PM with different colorations had a different element composition

21

22

23

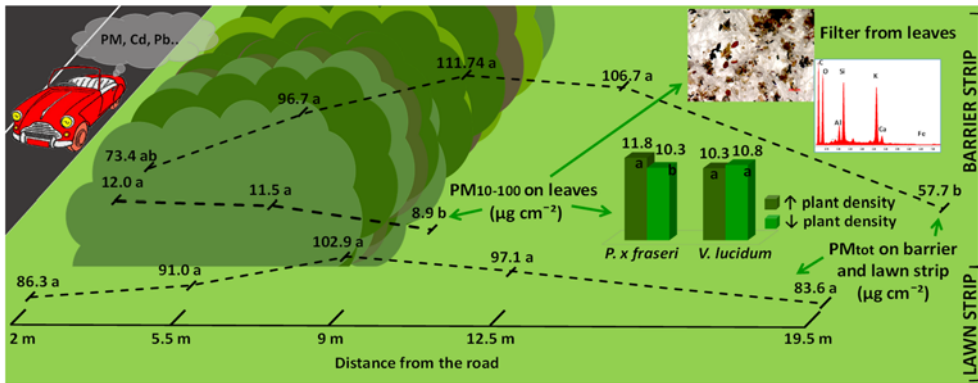
24

25

26

27

28 **Graphical abstract**



29

30 **Abstract**

31 Leaf deposition of PM₁₀₋₁₀₀, PM_{2.5-10}, PM_{0.2-2.5} and of 21 elements was investigated in a
 32 roadside vegetation barrier formed by i) two evergreen shrub species (*Photinia x fraseri*,
 33 *Viburnum lucidum*), with ii) two planting densities (0.5, 1.0 plant m⁻²), at iii) three distances
 34 from the road (2.0, 5.5, 9.0 m), at iv) two heights from the ground (1.5, 3.0 m), and on v)
 35 three dates (Aug, Sep, Oct).

36 The presence of black and brown on-leaf PM₁₀₋₁₀₀ and their element composition were
 37 detected by microscopy and image analysis. Pollutant deposition was also measured
 38 using passive samplers at five distances from the road (2.0, 5.5, 9.0, 12.5, 19.5 m) in the
 39 area of the barrier and in an adjacent lawn area.

40 *V. lucidum* had more PM_{2.5-10} and PM_{0.2-2.5} on leaves than *P. x fraseri*, while most elements
 41 were higher in *P. x fraseri*. Most pollutants decreased at increasing distances from the
 42 road and were higher at 1.5 m from the ground compared to 3.0 m.

43 Higher planting density in *P. x fraseri* enhanced the deposition of PM₁₀₋₁₀₀ and PM_{2.5-10},
 44 while in *V. lucidum*, the planting density did not affect the depositions.

45 Black PM₁₀₋₁₀₀ decreased a long distance from the road and was entirely composed of
 46 carbon and oxygen, which was thus identified as black carbon from fuel combustion.

47 The vegetation barrier had a higher deposition of most PM fractions at 5.5-12.5 m, while in
 48 the lawn area, depositions did not change. At 19.5 m, the PM₁₀₋₁₀₀ was 32% lower behind

49 the barrier than in the lawn area. In conclusion, the vegetation barrier changed the
50 deposition dynamics of pollutants compared to the lawn area. These results strengthen the
51 role of vegetation barriers and shrub species against air pollution and may offer interesting
52 insights for the use of new road green infrastructures to improve air quality.

53

54 **Keywords:** green infrastructure, particulate matter, leaf deposition, element, microscopy,
55 image analysis

56

57 **1. Introduction**

58 Urban air pollution is a threat for human health, causing nearly seven million premature
59 deaths per year throughout the world (WHO, 2014). Air quality is particularly poor in urban
60 areas because of the high level of emissions by anthropogenic activities (Sawidis et al.,
61 2011). Its negative impact is exacerbated by the fact that 54% of the world's population
62 live in these areas (United Nations, 2014). In Europe, it has been estimated that in 2015,
63 53% and 82% of urban populations were exposed to higher than WHO's recommendations
64 for daily levels of coarse (PM₁₀) and fine (PM_{2.5}) particulate matter (EEA, 2017).

65 Particulate matter is the most abundant air pollutant, consisting in a mixture of heavy
66 metals, elements, black carbon, soil and other substances (Thurston, 2008; Bell et al.,
67 2011). Improvement of air quality through the reduction of air pollutants is now a widely
68 accepted ecosystem service provided by urban vegetation (Simon et al., 2011; Sæbø et
69 al., 2012; Janhäll, 2015). The dry deposition of solid particles (hereafter, deposition) on
70 leaf surfaces is the basic mechanism of the beneficial action of plants on air quality
71 (Bealey et al., 2007; Nowak et al., 2013).

72 Leaf deposition is influenced by several factors such as the characteristics of particles
73 (concentration, diameter, composition, etc.), the vegetation (foliage density, porosity to air
74 fluxes, plant height, leaf characteristics, etc.), and the site (proximity of vegetation to

75 pollution source, meteorological conditions etc.) (Fowler et al., 2003; Freer-Smith et al.,
76 2005; Litschke and Kuttler, 2008; Petroff et al. 2008). The deposition of particles with a
77 diameter above one micrometer has been found to increase at higher air particle
78 concentrations and at increasing particle diameters (Fowler et al., 2003).

79 Increased foliar density leads to higher leaf deposition although very high density can
80 reduce the porosity of the canopy, thus limiting the air flux through the canopy and particle
81 deposition (Tiwary et al., 2005; Baldauf, 2017). Plant height influences air quality in
82 different ways depending on the characteristics of the planting site.

83 In open areas adjacent to roads, the improvement in air quality is more effective when the
84 canopy is taller than the impacting dust plume from traffic which in proximity to the road
85 can be around two meters (Etyemezian et al., 2003; Etyemezian et al., 2004). On the other
86 hand, in street canyons, trees with a large and thick canopy can also increase air pollution
87 concentrations at the pedestrian level because of a reduction in air pollutant dispersion
88 (Buccolieri et al., 2009).

89 The proximity of vegetation to the pollution source is another important factor increasing
90 leaf deposition (Pugh et al., 2012) which can limit the dispersion of pollutants to the
91 surrounding environment. Leaf deposition is also influenced by meteorological conditions,
92 for example rainfall can wash off leaf deposition (Nowak et al., 2006) to the ground, thus
93 reducing the possibilities of re-suspension in the atmosphere. High wind speed increases
94 not only deposition but also the re-suspension rate of deposited particles (Beckett et al.,
95 2000; Fowler et al., 2003).

96 With regard to leaf traits, evergreen plants are able to intercept higher quantities of
97 pollutants compared to deciduous species, especially during the winter season when the
98 concentration of air pollutants is generally higher (Pikridas et al., 2013). Among deciduous
99 species, plants with a longer in-leaf period are usually more effective. Species with smaller
100 leaves and more complex shoot structures are more efficient at capturing PM (Freer-Smith

101 et al., 2005). In addition, the presence of hairs and waxes has been associated with a
102 higher particulate deposition (Sæbø et al., 2012).

103 Several species, mostly trees native to northern environments (Aničić, et al., 2011; Popek
104 et al., 2017), have been investigated in terms of their capacity to remove air pollutants
105 (Dzierzanowski et al., 2011; Sæbø et al., 2012). However there have been few studies on
106 shrub species in southern Europe (Lorenzini et al., 2006; Mori et al., 2016).

107 Shrubs may represent a sound alternative to trees in reducing air pollution, especially in
108 contexts where tree planting is not possible because of a lack of space or due to law
109 enforcement (e.g. a ban on planting trees in proximity to roads) or because they are
110 detrimental to air quality (Buccolieri et al., 2009; Jeanjean et al., 2017).

111 Finally, the capacity of plants to reduce air pollution is influenced by the kind of green
112 infrastructure in which the vegetation is located (Abhijith et al., 2017). Roadside vegetation
113 barriers (hereafter, vegetation barriers) are green infrastructures consisting in rows of
114 shrubs and/or trees planted along roads (Abhijith et al., 2017; Baldauf, 2017). They screen
115 people living in neighboring areas from the drift of air pollutants from linear traffic (Al-
116 Dabbous and Kumar, 2014; Lin et al., 2016). The impact of vegetation barriers on air
117 quality has been assessed by experimental (Hagler et al., 2012) and modeling approaches
118 (Morakinyo and Lam, 2016) with contrasting results. While in the experimental study, no
119 clear effects of a roadside vegetation barrier on air quality were found, in the modeling
120 approach, beneficial influences of vegetation barriers were simulated.

121 Baldauf (2017) reviewed the characteristics of vegetation barriers that can increase the
122 capacity of air pollution mitigation. The height from the ground of vegetation barriers
123 should be higher than the initial dust plume derived from traffic; the recommended value
124 for this parameter is 4-5 m (Baldauf, 2017). The thickness of the vegetation barrier should
125 vary between 5 to 10 m and even more (Neft et al., 2016) depending on the foliar density.
126 An appropriate combination of thickness and foliar density should enable the suspended

127 particles to remain within the vegetation for a sufficient time to permit their removal from
128 the air while limiting air blocking (Neft et al., 2016). The vegetation coverage is also
129 crucial, given that pollutant fluxes can preferentially pass through vegetation gaps (e.g.,
130 spaces between plants) instead of through the vegetation barrier (Baldauf, 2017). In such
131 conditions, the effect of the vegetation barriers may be negatively affected. Finally, at least
132 a 50-m-length vegetation barrier is recommended in order to prevent pollutant fluxes from
133 passing laterally to the vegetation instead of passing through it (Baldauf, 2017).

134 Besides this growing body of research, more investigations are needed to better
135 understand and quantify the effects of roadside barriers on air pollution (Abhijith et al.,
136 2017). There is a lack of experimental data regarding the interaction between vegetation
137 barriers composed of evergreen shrubs, with different planting densities, and air pollutants
138 in the Mediterranean environment. A direct comparison between areas with and without
139 vegetation barriers thus may represents a novel approach.

140 In a previous study by our research group (Mori et al., 2015a), six evergreen shrub species
141 were characterized for the leaf deposition of PM and 21 elements mainly from traffic in a
142 peri-urban environment during a Mediterranean summer season.

143 Three out of six species (*Viburnum lucidum* L., *Photinia x fraseri* cv. Red Robin Dress and
144 *Elaeagnus x ebbingei* L.) were found to be more suitable for air pollution deposition
145 because of the higher growth (in terms of leaf area, leaf area index, plant biomass and
146 more favorable leaf traits) compared with the other species tested.

147 The aims of the present work was to study leaf deposition of three PM fractions (PM₁₀₋₁₀₀,
148 PM_{2.5-10} and PM_{0.2-2.5}) and of 21 elements (Al, As, Ba, Ca, Cd, Co, Cr, Cu, Fe, K, Li, Mg,
149 Mn, Mo, Ni, Pb, Sb, Se, Tl, V, Zn) in a vegetation barrier. In this study the barrier had
150 similar characteristics to those recommended in the literature in terms of height, length,
151 thickness and coverage (Baldauf, 2017). Several factors were studied: i) two different
152 planting densities ii) two species, iii) three distances from the road, iv) two heights from the

153 ground and v) three different sampling periods. *V. lucidum* L. and *Photinia x fraseri* Dress
154 were chosen as test plants based on our previous results (Mori et al., 2015a).

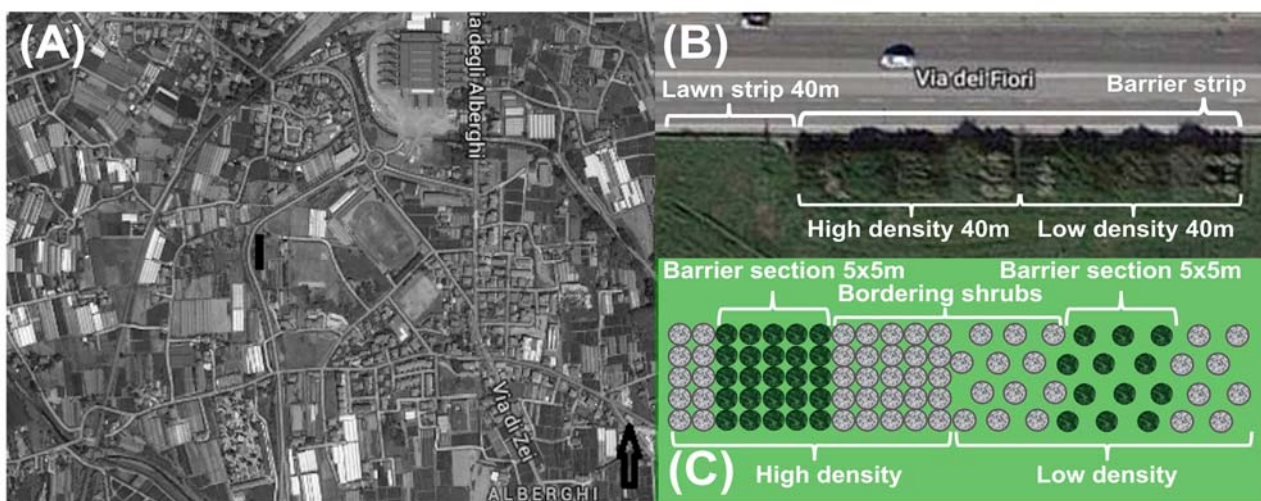
155 The influence of the vegetation barrier in the experimental area was also investigated by
156 direct comparison with an adjacent area characterized by lawn vegetation and by
157 measuring the deposition in i) both areas, in ii) three different sampling periods, and at iii)
158 five different distances from the road.

159

160 2. Materials and Methods

161 2.1 Experimental field

162 The experiment was conducted in Pescia, Tuscany, Italy (43°52'57.7992"N,
163 10°40'58.0692"E), (Fig. 1) in an experimental site, 35 km from the Tyrrhenian sea.



164

165 Fig. 1. Image of the area surrounding the experimental site taken from Mori et al. (2015a).

166 The orientation of the vegetation barrier is indicated with a dark rectangle, while the black
167 arrow indicates north (A). Aerial picture taken from Google Maps of the experimental area
168 comprising the barrier strip and the lawn strip (B). A part of the vegetation barrier with two
169 barrier sections (dark green circles) and the interposed shrub vegetation (light grey circles)
170 with the two different planting densities (C).

171 Annual rainfall is 901 mm, and minimum and maximum temperatures are 9.17°C and
172 19.8°C, respectively (thirty-year average data). Meteorological conditions during the
173 experiment (i.e. rainfall, wind speed, wind direction, relative humidity, and air temperature),
174 were monitored from 1 July 2016 (one month before the start of the sampling campaign) to
175 3 October 2016 (end of sampling campaign) using an in-situ meteorological station
176 iMetos® SD (Pessl Instruments, Weiz, Austria). The experimental field was located along
177 a 4-lane road which is the main access for vehicles to the center of the town. Traffic was
178 sampled manually similarly to Irga et al. (2015): vehicles passing in front of the barrier from
179 7:00 a.m. to 08:00 p.m. were counted manually on three different mid-week days.

180 The land use in the area was assessed as proposed by Irga et al. (2015), using satellite
181 images taken from Google maps within 100 m, 250 m, and 500 m radii from the
182 experimental site, which corresponded to 3.14, 19.6 and 78.6 ha, respectively. Images
183 were then analyzed with WinDIAS software (Dynamax Inc., USA) differentiating between
184 land surfaces occupied by buildings, streets, greenhouses, and green areas. Along the
185 road, in proximity to the study area, only agricultural activities (greenhouses and cultivated
186 fields) were present.

187

188 2.2 Experimental design

189 The vegetation barrier was parallel and downwind to the road with the predominant wind
190 blowing from the coast striking both the road and the vegetation barrier orthogonally (Fig.
191 1). In addition, the absence of obstacles between the vegetation barrier and the road,
192 together with a lack of road crossings or roundabouts near the vegetation barrier were
193 other important characteristics to ensure the uniformity of the experimental site in terms of
194 exposure to air pollution.

195 In March 2010, fifty 3-year-old *P. x fraseri* cv. Red robin and of *V. lucidum* plants (100
196 plants in total) were planted to form four different transects, of a vegetation barrier, as
197 previously described by Mori et al. (2015a).

198 The vegetation barrier was planted 2 m away from the road. Each barrier transect was
199 composed of 25 three-year-old plants per species, occupying an area of 5 by 5 m (with a
200 total of 100 plants per 100 m²). In winter 2015 (start of experiment), in one barrier transect
201 per species (2 out of 4 barrier transects), the density of plantation was homogeneously
202 reduced to 0.5 plant m⁻² (Fig. 1). On the same date, plants were cut back to a height of 3.5
203 m and laterally pruned in order to separate the plant crowns from each other. No other
204 pruning was carried out during the experiment in order to prevent any possible influence
205 on foliar deposition (see later).

206 The height of plants was generally higher than the initial dust plume from traffic (2 m),
207 (Etyemezian et al., 2003) and similar to those recommended by Baldauf (2017). The heights
208 of all plants were measured again at the end of the experiment. The sides of each barrier
209 transect that were parallel to the road (roadside and opposite-roadside) were free from any
210 physical obstacles, while orthogonal roadsides verged with other barrier transects made
211 up of shrubs of an equal height (3.5 m) compared with the studied species. The aim of this
212 arrangement was to limit the intrusion of air fluxes laterally to the barrier transects and to
213 favor air passing from the road within the barrier. The length of the total vegetation barrier
214 (studied and non-studied barrier transects) was 80 meters in line with the recommendation
215 reported by Baldauf (2017). In addition, due to the homogeneous and staggered
216 distribution of plants within the different barrier transects, no free gaps were present.

217 A lawn area behind (9.0 to 19.5 m from the road) and adjacent (2.0 to 19.5 m from the
218 road) to the vegetation barrier was also considered for measurements. The height of the
219 grass in the lawn area was maintained below 20 cm tall throughout the experiment in order
220 to not interfere with the passive samplers (see below). The area from 2.0 m to 19.5 m from

221 the road in which the vegetation barrier was present was defined as the “barrier strip”,
222 while the area entirely characterized by lawn vegetation was defined as the “lawn strip”.
223 The average leaf area index (LAI) of the various barrier transects was monitored using a
224 ceptometer (AccuPAR LP-80, Decagon Devices, Inc., WA, USA). Data were recorded at 1
225 m height, positioning the linear optical sensor of the instrument parallel to the ground
226 below each plant and between plants in two different orthogonal directions, following the
227 ceptometer manual.

228 The total leaf area of the barrier transects was estimated by multiplying the mean LAI of
229 each transect (2 species x 2 planting densities) by the corresponding projection of the
230 canopy. Passive samplers (30) were placed in the barrier and in the lawn strip, at 2.0, 5.5,
231 9.0, 12.5 and 19.5 m from the road in order to collect PM_x and element deposition. The
232 passive samplers were positioned: i) directly exposed to traffic (2.0 m from the road), ii) in
233 the middle of the vegetation barrier (5.5 m from the road), iii) behind the barrier (9.0 m
234 from the road), iv) as position (iii) plus the barrier height (9.0 + 3.5 = 12.5 m from the road),
235 as position (iii) plus 3 times the barrier height (9.0 + 10.5 = 19.5 m from the road). The
236 passive samplers were created using a wooden rod (1.5 m length) as a vertical support on
237 which a rigid plastic plate (25 x 15 cm) was horizontally mounted. Two
238 polytetrafluoroethylene membranes (PTFE) (i.e., one used to collect PM_x deposition and
239 one used for the element deposition) were placed on the central part of the plastic plate.
240 The stability of the PTFE membrane was insured by four PTFE screws and washers,
241 which were positioned with millimetric precision thereby covering the same surface of
242 membranes among samplers.

243 A fiberglass sheet (50 x 20 cm) was mounted on the top of the passive samplers by fixing
244 the short sides of the sheet on the reciprocal sides of the plastic plates to protect the PTFE
245 membranes from rainfall, while ensuring the passage of air flows in the orthogonal
246 direction with respect to the longer side. Passive samplers were then positioned with the

247 long side of the plastic plate parallel to the road. The distance (in height) between the
 248 fiberglass sheet and the PTFE membranes was 20 cm. Passive samplers were positioned
 249 in order to maintain PTFE membranes 1 meter from the ground, which was deemed a
 250 good compromise for collecting pollutant deposition at ground level while limiting
 251 contamination from the soil.

252 A preliminary test was performed to verify deposition homogeneity among samplers during
 253 a one-month period of exposure to traffic, 2.0 m from the road, in the same experimental
 254 location.

255 To determine the composition in elements, approximately 500 g of topsoil were collected
 256 from the 0 – 10 cm soil layer at five different distances from the road (2.0 m, 5.5 m, 9.0 m,
 257 12.5 m, 19.5 m) in both the barrier and lawn strips (three replicates for a total of 30
 258 samples). During sampling, any visible organic debris that could potentially affect the
 259 concentration of elements in the soil was avoided (Skrbìc et al., 2012). To determine the
 260 element concentration, topsoil samples were processed following the protocol reported in
 261 Mori et al., (2015a).

262

263 2.3 PM_x and elements deposition – sampling

264 Leaf samples of roughly 400 cm² each (Dzierzanowski et al., 2011; Saebo et al., 2012)
 265 were collected in two replicates as reported in Tab. 1.

266

267 Tab. 1. Type of collected samples, fixed factors per kind of collected sample, number of
 268 levels per fixed factor, number of samples per level of fixed factor, and description of the
 269 levels of each fixed factor.

Type of sample (variable factors)	Fixed factors	Levels (N°)	Samples per level (N°)	Description
Leaf deposition (PM _x and elements)	Species	2	72	<i>V. lucidum</i> ; <i>P. x fraseri</i>
	Planting density	2	72	0.5 plants m ⁻² ; 1.0 plants m ⁻²
	Distance from the road	3	48	2.0 m; 5.5 m; 9.0 m
	Height from the ground	2	72	1.5 m; 3.0 m

	Sampling dates	3	48	01 Ago 2016; 01 Sept 2016; 03 Oct 2016
Deposition on passive samplers (PM _x and elements)	Experimental strips	2	45	Barrier strip; lawn strip
	Distance from the road	5	18	2.0 m; 5.5 m; 9.0 m; 12.5 m; 19.5 m
	Sampling dates	3	30	01 Ago 2016; 01 Sept 2016; 03 Oct 2016
Percentage of filter surface occupied by PM ₁₀₋₁₀₀	Species	2	216	<i>V. lucidum</i> ; <i>P. x fraseri</i>
	Planting density	2	216	0.5 plants m ⁻² ; 1.0 plants m ⁻²
	Distance from the road	3	144	2.0 m; 5.5 m; 9.0 m
	Height from the ground	2	216	1.5 m; 3.0 m
	Sampling dates	3	144	01 Ago 2016; 01 Sept 2016; 03 Oct 2016
	Color of particles	2	216	Black; brown

270

271 A total of 144 samples were collected for PM_x and another 144 for elements, based on
272 previous findings reported by Mori et al., 2015a. The sampling period (01 August 2016 - 03
273 October 2016) was based on previous experience (Mori et al., 2015a) and in particular on
274 the need to carry out measurements both during the dry summer season and the start of
275 the rainy season (autumn). This enabled us to verify the influence of planting density,
276 species, height of leaves etc. under different climatic conditions. Samples of the current
277 season and healthy leaves were collected maintaining a distance of at least 1.5 m from the
278 adjacent barrier transect in order to reduce contamination/side effects. However, to limit
279 contamination of samples, samples were collected using disposable gloves and harvesting
280 leaves from the petioles to prevent contact with the leaf blade. After sampling, leaves were
281 placed in disposable paper bags before being processed in the laboratory.

282 PTFE membranes were sampled on the same days as leaves, with a total of 90
283 membranes for PM_x and another 90 membranes for elements collected throughout the
284 entire experiment (Tab. 1). PTFE membranes were collected and replaced on the same
285 day using plastic tweezers. Once removed, each PTFE membrane was placed into a 50 ml
286 plastic tube. Each sampling was carried out at least 10 days after the last rainfall.

287

288 2.4 PM_x deposition - determination

289 The original protocol by Dzierzanowski et al. (2011) for PM_x leaf deposition analysis was
290 modified as follows. Three different filters with different retention capacities were used

291 (type 91 - retention 10 μm , type 42 – retention 2.5 μm and PTFE membrane - retention 0.2
292 μm), (Whatman, UK). Each filter was firstly dried at 60°C for 30 minutes in a KCW-100
293 drying chamber (PREMED, Poland) and then left for 60' at a constant relative air humidity
294 (50 %) for weight stabilization. Filters were then pre-weighed on BCA 2005 scales (Orma
295 s.r.l., Italy). Each leaf sample was washed for 60'' with 150 ml of deionized water under
296 agitation. The washing solution was then filtered through a metal sieve (Haver and
297 Boecker, Germany) in order to eliminate particles larger than 100 μm , and then
298 sequentially filtered using the three filters in the increasing order of retention capacity (10
299 μm , 2.5 μm , 0.2 μm).

300 Filtration was carried out using an apparatus equipped with a 47 mm glass filter funnel
301 (Scharlau, Scharlab, S.L., Barcelona, Spain) connected to a MV-50 vacuum pump
302 (Comecta-Ivymen, Spain). Immediately before filtration, PTFE membranes were
303 moistened with a few droplets of isopropyl alcohol to break the surface forces and speed
304 up the process. After filtration, filters were dried, left to stabilize and then weighed again.

305 At the end of the entire filtration procedure, three fractions of PM_x were collected: (1)
306 large: 100-10 μm (PM_{10-100}), (2) coarse: 10–2.5 μm ($\text{PM}_{2.5-10}$), and (3) fine: 2.5–0.2 μm
307 ($\text{PM}_{0.2-2.5}$). After washing, the leaf area of each sample was measured using an RS 2 XA
308 illumination and camera system (Haiser, Germany) and an A3 Lightbox (G.C.L., UK) with
309 WinDIAS software (Dynamax Inc., USA). The protocol for PM_x deposition in the barrier and
310 lawn strips was the same as the one used for leaf samples, except for the washing phase
311 of PTFE membranes which was carried out directly in the 50 ml plastic tube used for
312 collection using 50 ml of deionized water. The results of PM_x deposition on leaves and in
313 the barrier and lawn strips were expressed per unit area of leaf and PTFE membranes,
314 respectively. On the same day, one blank (consisting of 150 ml for leaf samples, and 50 ml
315 for PTFE membrane samples) every 20 samples, was filtered with the same protocol as
316 outlined above. The blank values were negligible.

317

318 2.5 Element deposition - determination

319 Leaf samples were washed using the same protocol as for PM_x determination, but only
320 filtration with the metal sieve (Haver and Boecker, Germany) was carried out. The washing
321 solution (150 ml) was collected in a beaker and reduced up to 10 ml at 70°C. The
322 concentrated solution was then digested using a heating digester (DK20, Velp® Scientifica,
323 Italy), at 170°C per 120 min adding 12 ml of a mixture of HNO₃ (65%) and H₂O₂ (30%)
324 (10:2) V/V. A water-cooling system was applied to reduce the loss of elements by
325 evaporation and to prevent samples from drying. Finally, the volume was adjusted to 25 ml
326 with deionized water.

327 The concentration of 21 elements (Al, As, Ba, Ca, Cd, Co, Cr, Cu, Fe, K, Li, Mg, Mn, Mo,
328 Ni, Pb, Sb, Se, Tl, V, Zn) was determined by an Inductively Coupled Plasma – Optical
329 Emission Spectrometer – (Optima 7000, Perkin Elmer, Massachusetts, U.S.). PTFE
330 membranes were processed with the same protocol used for leaves, apart from the
331 volume of deionized water used for washing (50 ml). The protocol used for the digestion
332 phase, reported by Mori et al. (2015a; 2015b), was modified in terms of the temperature
333 and duration. One blank (consisting of 10 ml of reduced deionized water) every 20
334 samples, was digested with the same aforementioned protocol, on the same day of
335 analysis. Blank values were negligible.

336 The results of the element deposition were expressed per unit area of leaf surface or
337 PTFE membrane surface. Total leaf deposition of PM_x and elements on vegetation barrier
338 transects (two species for two different planting densities), were calculated by multiplying
339 the mean leaf deposition per unit leaf surface of each transect by the corresponding total
340 leaf area.

341

342 2.6 Microscope analysis

343 From each paper filter (type 91) used for the analysis of PM₁₀₋₁₀₀ leaf deposition (see 2.4
344 section), three images were taken at 10x magnification, using an optical confocal
345 microscope (Axioskop 40, Zeiss, Germany) equipped with an Axiocam camera (MR 5,
346 Zeiss) and Axiovision Rel.4.6 software (Zeiss) with a total number of 432 images (Tab. 1).
347 Images were then analyzed using an RS 2 XA illumination and camera system (Haiser,
348 Germany) and A3 Lightbox (G.C.L., UK) with WinDIAS software (Dynamax Inc., USA) in
349 order to differentiate between PM₁₀₋₁₀₀ with different colorations (black or brown), and to
350 calculate the relative percentage of paper filter surface occupied by different colored PM<sub>10-
351 100.</sub>

352 Nine PM₁₀₋₁₀₀ paper filters, already used for optical microscope observations,
353 representative of different sampling periods and distances from the road, were observed
354 using a Quanta 200, Environmental Scan Electronic Microscope (ESEM), FEI Thermo
355 Fisher Scientific (Oregon, USA), at 80–400x magnification. In addition, to investigate the
356 element composition, X-ray microanalysis was carried out on two black and two brown
357 particles per filter by an EDS-X-ray microanalysis system (EDAX Genesis, AMETEK,
358 Mahwah, NJ, USA). Observations of the leaf surfaces of the two species were also carried
359 out with ESEM in order to assess the presence of waxes and trichomes on the upper and
360 lower leaf surface. Only current season and fully expanded leaves were considered for the
361 above analysis.

362

363 2.7 Data analyses and statistics

364 Multi-way ANOVA was applied to i) data of leaf deposition; ii) barrier and lawn strip
365 deposition and; iii) percentages of PM₁₀₋₁₀₀ filter surfaces occupied by black and brown
366 particles. The number of fixed factors (and thus of the number of ways of the ANOVA), per
367 measured variable are reported in Tab. 1. Significant interactions between factors were
368 subsequently investigated by one-way ANOVA. Mean values were separated by Tukey's

369 (HSD) post-hoc test ($P \leq 0.05$). The outliers were identified by a Box and Wisker plot, and
370 removed from the dataset.

371 A correlation analysis between the leaf deposition and climatic parameters (air
372 temperature, wind speed and precipitations) was performed using Pearson product-
373 moment coefficients..

374 Principal component analysis (PCA) was performed in order to: i) group the studied air
375 pollutants (PM_x and elements on leaves) explaining most of the experimental variability,
376 and ii) obtain a graphical representation of the influence of the various factors (species,
377 sampling date, planting density) in inducing variance within the model. The analysis was
378 performed on the basis of a correlation matrix as suggested by (Catoni and Gratani, 2014).
379 Each individual air pollutant was assigned to a different group on the basis of the principal
380 component with the highest component weight in absolute value. All the statistical
381 analyses were carried out using Statgraphics Centurion XV (Stat Point, Inc., Herndon, VA,
382 USA), while the graphics were drawn with SigmaPlot 11.0, Systat Software Inc. (San Jose,
383 California, USA).

384

385 **3. Results**

386 3.1 Experimental field

387 The meteorological data recorded throughout the entire experiment were representative of
388 the typical Mediterranean climate, with high temperatures and almost no rainfall between
389 July and August, followed by an increase in rainfall events and a decline in air temperature
390 and in wind speed from September to October (Tab. 2A). The surrounding land was mainly
391 used for agriculture and green areas in general (59.5%) (Tab. 2B), roads and parking
392 ranked second with 29.8%, while buildings occupied the remaining 10.7%. A mean
393 number of 10,844 vehicles per day passed on the road adjacent to the vegetation barrier
394 between 7:00 a.m. and 08:00 p.m. Similarly to Hagler et al. (2012), and Irga et al. (2015),

395 the fleet mix was not quantified for this study. Data regarding element composition in
 396 topsoil (data not shown) were similar to those from the same area reported in Mori et al.
 397 (2015a). In addition, no differences between the barrier and lawn strip and between
 398 distances from the road were found with the exception of Ca, which decreased significantly
 399 at increasing distances (data not shown).

400

401 Tab. 2 Meteorological data at the experimental area averaged in the different sampling
 402 periods (A). Land use partitioning (%) within 100, 250 and 500 m radii distant from
 403 roadside vegetation barrier (B).

404

(A)	Period	Air temperature (°C)	Rainfall (mm)	Wind velocity (m s ⁻¹)	Wind direction	Air RH (%)
	1 Jul – 1 Aug 16	24.25	1.6	0.88	WSW	57.62
	2 Ago – 1 Sep 16	23.63	3.2	0.81	SW	55.24
	2 Sep – 3 Oct 16	20.71	24.3	0.45	WSW	65.57
(B)	Radii distance (m)	Green areas and greenhouses (%)	Buildings (%)	Roads and parking (%)		
	100	68.3	4.8	26.9		
	250	61.5	9.6	28.9		
	500	48.7	17.6	33.7		

405

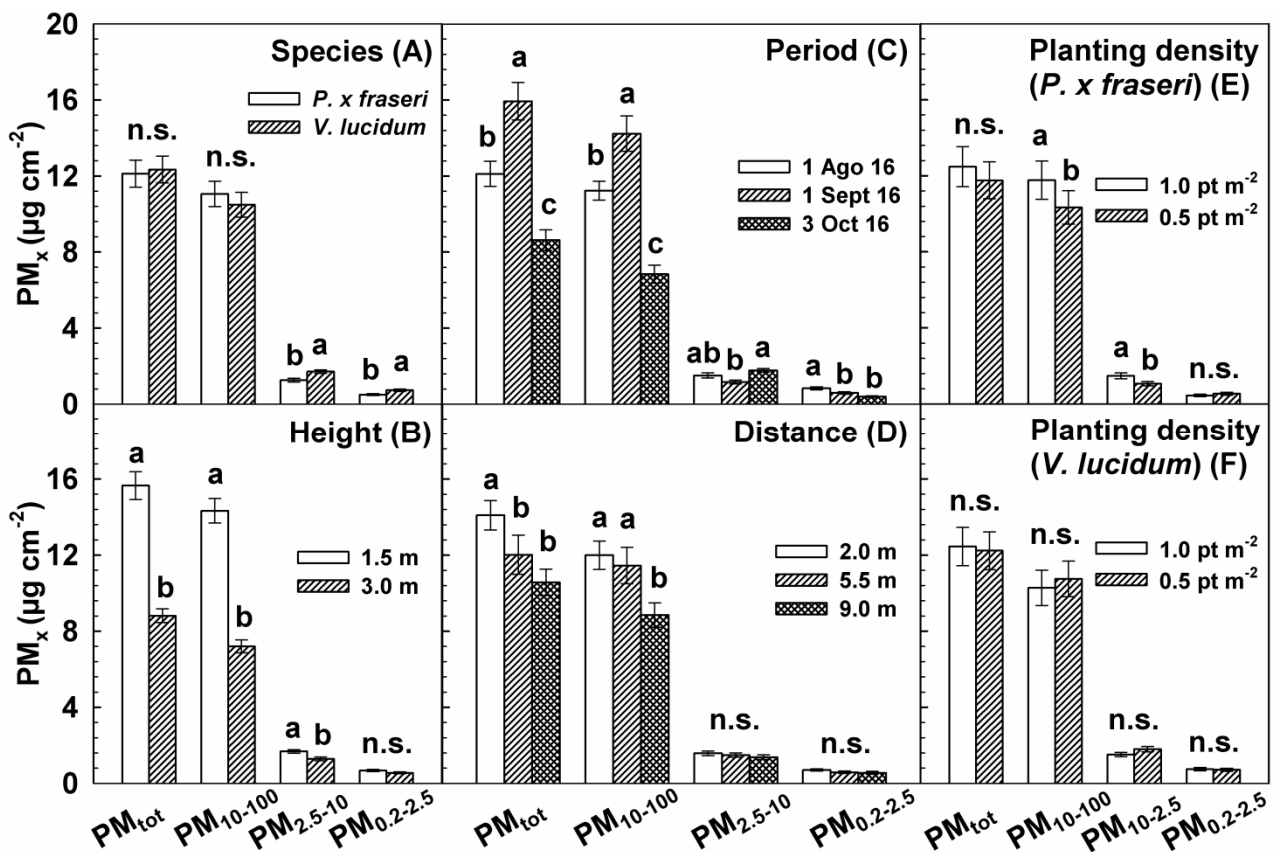
406 3.2 Plant growth

407 Planting density affected LAI in the barrier transects with *P. x fraseri* ($P < 0.001$), with larger
 408 LAI developed at the higher planting density (8.07 ± 1.08 SD) compared with the lower
 409 planting density (4.82 ± 2.11 SD), but had no significant effect on *V. lucidum* ($0.5 \text{ pt m}^{-2} =$
 410 7.68 ± 1.73 SD; $1.0 \text{ pt m}^{-2} = 8.72 \pm 1.45$). The height of plants increased on average by
 411 8.5% from winter 2015 to the end of the experiment, without significant differences
 412 between species and planting densities (data not shown).

413

414 3.3 PM_x deposition per unit leaf area

415 In *P. x fraseri*, PM_{2.5-10} and PM_{0.2-2.5} leaf depositions were lower compared with *V. lucidum*,
 416 while no differences were detected for the other PM fractions (Fig. 2A). Leaf deposition of
 417 PM_{tot}, PM₁₀₋₁₀₀ and PM_{2.5-10} at 3.0 m height from the ground were 43.7%, 49.8% and
 418 23.2%, lower than the deposition at 1.5 m (Fig. 2B). PM_{tot} and PM₁₀₋₁₀₀ leaf deposition
 419 increased by 31.5% and 26.7%, respectively, from August to September and then
 420 decreased in October by 28.8% and 39.1% (Fig. 2C). On the other hand, PM_{2.5-10} leaf
 421 deposition did not change significantly from August to September but increased by 17.9 %
 422 from September to October. PM_{0.2-2.5} decreased, on average, by 40.5% from August to
 423 October. PM_{tot} and PM₁₀₋₁₀₀ leaf deposition decreased by 25.0% and 26.3% respectively
 424 from 2.0 to 9.0 m from the road, while no differences for the smaller fractions were found
 425 (Fig. 2D). Higher planting density in *P. x fraseri* increased PM₁₀₋₁₀₀ and PM_{2.5-10} leaf
 426 deposition by 13.8% and 38.3%, respectively, compared with the lower planting density,
 427 while no other differences were found for the other fractions in either species (Fig. 2E, 2F).



428

429 Fig. 2. Leaf deposition per unit leaf surface of different fractions of PM_x for: (1A) two
430 different shrub species (*P. x fraseri* and *V. lucidum*) (n = 72), (1B) two different heights
431 from the ground (1.5 m and 3.0 m) (n=72), (1C) three different sampling periods (01 Aug
432 2016, 1 Sep 2016 and 03 Oct 2016) (n = 48), (1D) three different distances from the road
433 (2.0 m, 5.5 m and 9.0 m) (n = 48), (1E-F) two different planting densities (0.5 plants m⁻²
434 and 1.0 plants m⁻²) in (E) *P. x fraseri* (n = 36) and in (F) *V. lucidum* (n = 36). Columns are
435 means (µg cm⁻²) ± SE. Different letters indicate significant differences for the same PM_x
436 fraction at P = 0.05 using Tukey's (HSD). n.s. indicates no significant difference.

437

438 3.4 Element deposition per unit leaf area

439 Lead, Sb, Se and Tl were not detected in most leaf samples and were removed from the
440 dataset (Tab. 3). The other elements were found in the following rank order: Ca > Fe > Al
441 > Mg > K > Mn > Zn > Cu > Ba > V > As > Ni > Cr > Li > Mo > Co > Cd. *P. x fraseri*
442 showed a higher leaf deposition in 13 out of 17 elements compared with *V. lucidum*, while
443 no significant differences were found for Al, Cr, Cu and Zn (Tab. 3). Leaf deposition of all
444 elements changed between sampling periods apart from Mn. Twelve out of 17 elements
445 (Al, Ba, Co, Cr, Cu, Fe, K, Li, Mg, Ni, V, Zn) showed an increase from Aug to Sep, and
446 thereafter a decrease in Oct (Tab. 3), whereas As, Cd, and Mo increased during the
447 sampling periods (Tab. 3). Planting density influenced leaf deposition in 10 out of 17
448 elements, thereby increasing Al, Ba, Ca, Cr, Cu, Fe, K, Mg, and V (Tab. 3). The distance
449 from the road had an effect on leaf deposition in 12 out of 17 elements, with generally
450 higher values at 2.0 m from the road compared with values at 9.0 m (Tab. 3). The height
451 from the ground affected leaf deposition in 14 out of 17 elements. In 12 cases (Al, Ba, Ca,
452 Co, Cr, Cu, Fe, K, Mg, Ni, V, Zn), values were higher at 1.5 m compared with 3.0 m, while
453 for As and Cd an opposite trend was observed (Tab. 3).

454

455

456 Tab. 3 Leaf deposition per unit leaf surface of different elements (Al, As, Ba, Ca, Cd, Co,
457 Cr, Cu, Fe, K, Li, Mg, Mn, Mo, Ni, V, Zn) for: i) two different shrub species (*P. x fraseri* and
458 *V. lucidum*) (n = 72), ii) three different sampling periods (01 Aug 16, 1 Sep 16 and 03 Oct
459 16) (n = 48), iii) two different planting densities (0.5 plants m⁻² and 1.0 plants m⁻²) (n = 72),
460 iv) three different distances from the road (2.0 m, 5.5 m and 9.0 m) (n = 48), v) two
461 different heights from the ground (1.5 m and 3.0 m) (n = 72). Values are means (µg cm⁻²).

	Al	As	Ba	Ca	Cd	Co	Cr	Cu	Fe	K	Li	Mg	Mn	Mo	Ni	V	Zn
Species (Sp)																	
<i>P. x fraseri</i>	0.20 a	0.0013 a	0.0049 a	0.67 a	0.00020 a	0.00029 a	0.0010 a	0.0082 a	0.25 a	0.16 a	0.00094 a	0.21 a	0.02 a	0.00033 a	0.0012 a	0.0017 a	0.020 a
<i>V. lucidum</i>	0.18 a	0.0011 b	0.0042 b	0.59 b	0.00018 b	0.00026 b	0.0009 a	0.0073 a	0.23 b	0.12 b	0.00080 b	0.16 b	0.03 b	0.00030 b	0.0011 b	0.0015 b	0.0208 a
Period (Pd)																	
01 Ago 16	0.21 b	0.0011 b	0.0041 b	0.74 a	0.00017 b	0.00028 b	0.0009 b	0.0058 b	0.25 b	0.13 b	0.00084 b	0.20 b	0.02 a	0.00029 b	0.0011 b	0.0018 b	0.0209 b
01 Sept 16	0.25 a	0.0012 b	0.0063 a	0.81 a	0.00019 a	0.00030 a	0.0012 a	0.0109 a	0.33 a	0.17 a	0.00095 a	0.23 a	0.03 a	0.00032 ab	0.0013 a	0.0022 a	0.0250 a
03 Oct 16	0.10 c	0.0013 a	0.0033 c	0.34 b	0.00020 a	0.00024 c	0.0007 c	0.0065 b	0.15 c	0.11 c	0.00082 b	0.12 c	0.02 a	0.00034 a	0.0010 b	0.0008 c	0.0164 c
Density (Dt)																	
1.0 pt m ⁻²	0.21 a	0.0012 a	0.0050 a	0.66 a	0.00018 a	0.00028 a	0.0010 a	0.0079 a	0.26 a	0.14 a	0.00088a	0.19 a	0.02 a	0.00031 a	0.0012 a	0.0017 a	0.0212 a
0.5 pt m ⁻²	0.18 b	0.0012 a	0.0042 b	0.60 b	0.00018 a	0.00027 a	0.0009 b	0.0076 b	0.22 b	0.14 b	0.00086 a	0.18 b	0.03 a	0.00031 a	0.0011 a	0.0015 b	0.0203 a
Distance (Dc)																	
2.0 m	0.20 a	0.0012 a	0.0048 a	0.77 a	0.00020 a	0.00029 a	0.0011 a	0.0092 a	0.27 a	0.13 a	0.00090 a	0.21 a	0.02 a	0.00034 a	0.0012 a	0.0017 a	0.0261 a
5.5 m	0.20 a	0.0012 a	0.0047 a	0.62 b	0.00018 a	0.00028 ab	0.0010 a	0.0079 b	0.26 a	0.14 a	0.00086 b	0.18 b	0.02 a	0.00031 ab	0.0011 ab	0.0016 a	0.0210 b
9.0 m	0.17 b	0.0012 a	0.0041 a	0.50 c	0.00019 a	0.00026 b	0.0008 b	0.0061 c	0.20 b	0.14 a	0.00085 b	0.17 b	0.02 a	0.00030 b	0.0011 b	0.0014 b	0.0151 c
Height (Ht)																	
1.5 m	0.25 a	0.0011 b	0.0056 a	0.80 a	0.00018 b	0.00030 a	0.0012 a	0.0098 a	0.33 a	0.16 a	0.00088 a	0.23 a	0.03 a	0.00031 a	0.0012 a	0.0021 a	0.0245 a
3.0 m	0.14 b	0.0013 a	0.0035 b	0.46 b	0.00020 a	0.00025 b	0.0007 b	0.0057 b	0.16 b	0.12 b	0.00086 a	0.14 b	0.02 a	0.00033 a	0.0010 b	0.0011 b	0.0170 b
Significance*																	
Sp	0.085	0.001	0.009	<0.001	0.002	<0.001	0.422	0.005	0.027	<0.001	<0.001	<0.001	0.046	<0.001	0.004	<0.001	0.922
Pd	<0.001	0.001	<0.001	<0.001	0.004	<0.001	<0.001	<0.001	<0.001	<0.001	<0.001	<0.001	0.184	0.002	<0.001	<0.001	<0.001
Dt	<0.001	0.867	0.002	0.010	0.693	0.393	0.004	0.421	<0.001	0.178	0.157	0.007	0.061	0.919	0.159	<0.001	0.473
Dc	0.001	0.770	0.077	<0.001	0.230	0.001	<0.001	<0.001	<0.001	0.379	0.050	<0.001	0.837	0.020	0.001	<0.001	<0.001
Ht	<0.001	<0.001	<0.001	<0.001	0.012	<0.001	<0.001	<0.001	<0.001	<0.001	0.234	<0.001	0.075	0.031	<0.001	<0.001	<0.001
Sp x Dc	0.378	0.082	0.772	0.578	0.300	0.248	0.900	0.440	0.318	0.458	0.078	0.102	0.024	0.340	0.349	0.134	0.282

Sp x Dt	0.244	0.767	0.086	0.143	0.953	0.791	0.380	0.549	0.566	0.170	0.727	0.164	0.005	0.909	0.769	0.221	0.201
---------	-------	-------	-------	-------	-------	-------	-------	-------	-------	-------	-------	-------	-------	-------	-------	-------	-------

462

463 *P-Values are reported for all factors and for interactions. Different letters indicate significant differences within the same factor and
464 element at $P = 0.05$ using Tukey's (HSD).

465 3.5 Total leaf deposition per barrier transect

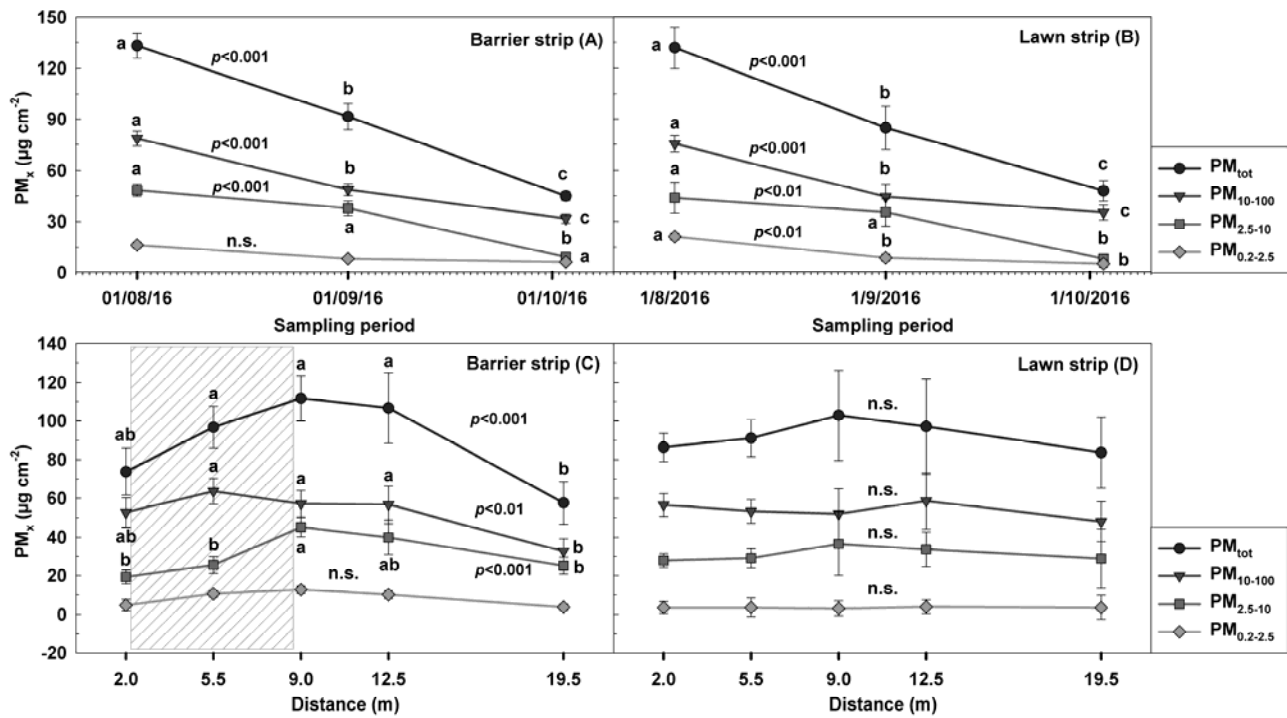
466 The barrier transects composed of *P. x fraseri* had a lower total leaf deposition compared
467 with *V. lucidum* in 12 out of 17 elements (Al, As, Cd, Co, Cr, Cu, Fe, Li, Mn, Mo, Ni, Zn), in
468 PM_{tot} , $PM_{2.5-10}$ and in $PM_{0.2-2.5}$, while for the other air pollutants, no significant differences
469 were found (Tab. A). A higher planting density increased total leaf deposition in all cases
470 apart from Mn and $PM_{0.2-2.5}$ (Tab. A). Generally, *P. x fraseri* at 0.5 pt m⁻² showed the lowest
471 leaf deposition in most elements, in PM_{tot} and in PM_{10-100} (Tab. A), while planting density
472 in *V. lucidum* did not show a clear effect on leaf deposition.

473

474 3.6 PM_x deposition in the barrier and lawn strip

475 PM_x deposition decreased from August to October (PM_{tot} = -65 %; PM_{10-100} = -56 %; $PM_{2.5-10}$
476 $= -81$ %; $PM_{0.2-2.5}$ in lawn strip = -76 %), except for $PM_{0.2-2.5}$ in the barrier strip which did
477 not vary over time (Fig. 3A, B). The distance from the road significantly influenced
478 deposition depending on the PM_x fraction and strip type (Fig. 3C, 2D). In the barrier strip,
479 the deposition of PM_{tot} , PM_{10-100} and $PM_{2.5-10}$ showed a non-linear trend, increasing from
480 2.0 m to 12.5 m and decreasing thereafter with significantly lower values at a 19.5 m
481 distance (Fig. 3C). The deposition in the lawn strip however, showed a linear trend without
482 any significant reduction (Fig. 3D). The barrier strip at 19.5 m showed a 31% and 32%
483 lower deposition for PM_{tot} and PM_{10-100} respectively, compared with the lawn strip at
484 $P < 0.05$, while no other differences between the same distance in the different strips were
485 found.

486



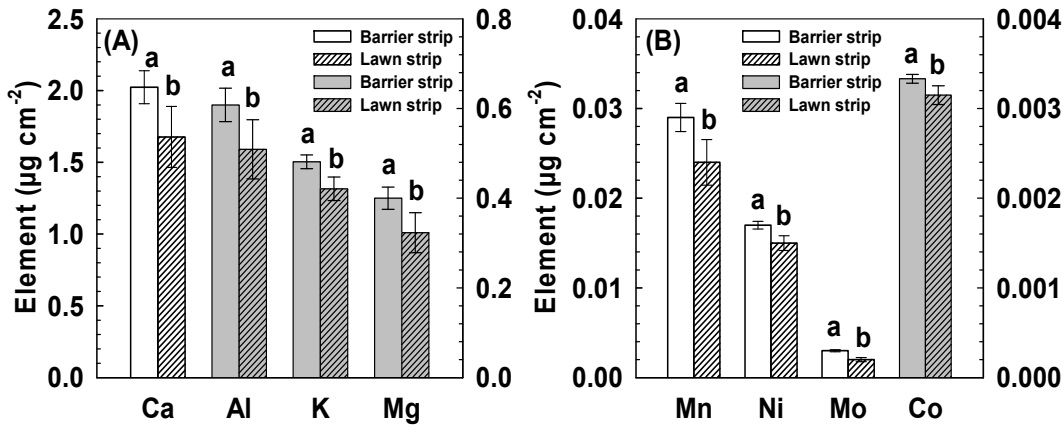
487

488 Fig. 3. Deposition in the barrier (A) and lawn (B) strip of different PM_x fractions per unit
 489 PTFE membrane area in three different sampling periods. Deposition in the barrier (C) and
 490 lawn (D) strip of different PM_x fractions at five different distances from the road. The
 491 rectangle in Fig. 3C indicates the lateral section of the vegetation barrier. Values are
 492 means ($\mu\text{g cm}^{-2}$) \pm SE. Different letters indicate significant differences within the same PM_x
 493 fraction at $P=0.05$ using Tukey's test (HSD). n.s. indicates no significant difference.

494

495 3.7 Element deposition in the barrier and lawn strip

496 Five out of 21 analyzed elements (Pb, Sb, Se, Tl and V) were not detected in the majority
 497 of samples and were therefore removed from the dataset. Similarly to the leaf deposition
 498 findings, elements showed different concentrations in the following rank order: $\text{Ca} > \text{Fe} >$
 499 $\text{Al} > \text{K} > \text{Zn} > \text{Mg} > \text{Mn} > \text{As} > \text{Ba} > \text{Ni} > \text{Cu} > \text{Li} > \text{Cr} > \text{Cd} > \text{Co} > \text{Mo}$ (Tab. 4). Barrier and
 500 lawn strips differed in the deposition of 8 out of 16 elements (Ca, Al, K, Mg, Mn, Ni, Mo,
 501 Co), with higher values in the barrier strip compared with the lawn strip (Fig. 4).



502

503 Fig. 4. Deposition per unit PTFE membrane area of Ca, Al, K, Mg (A) and Mn, Ni, Mo, Co
 504 (B) in the barrier strip and in the lawn strip. Ca, Mn, Ni, and Mo refer to left y axes; while
 505 Al, K, Mg, and Co refer to right y axes. Values are means ($\mu\text{g cm}^{-2}$) \pm SE. Different letters
 506 indicate significant differences within the same element at $P= 0.05$ using Tukey's test
 507 (HSD).

508

509 Element deposition in the barrier and lawn strips changed similarly over time (Tab. 4). In
 510 10 out of 17 elements (Al, Ba, Ca, Cd, Cr, Fe, K, Mg, Mn, Mo), there was a decrease from
 511 the August to September and an increase from September to October. Element deposition
 512 decreased significantly at increasing distances from the road with a higher decreasing rate
 513 in the barrier strip than in the lawn strip (Tab. 4).

514

515 Tab. 4. Deposition per unit PTFE membrane area of 16 elements (Al, As, Ba, Ca, Cd, Co,
 516 Cr, Cu, Fe, K, Li, Mg, Mo, Ni, V, Zn) in the barrier strip (A) ($n = 45$) and in the lawn strip (B)
 517 ($n = 45$) in i) three different sampling periods (1 Aug 16, 1 Sep 16 and 3 Oct 16) ($n = 15$)
 518 and at ii) five different distances from the road (2.0 m, 5.5 m, 9.0 m, 12.5 m, 19.5 m) ($n =$
 519 9). Values are means ($\mu\text{g cm}^{-2}$).

(A) Barrier strip

	Al	As	Ba	Ca	Cd	Co	Cr	Cu	Fe	K	Li	Mg	Mn	Mo	Ni	Zn
Period (Pd)																
01 Aug 16	0.83 a	0.030 a	0.016 a	2.44 a	0.0043 a	0.003 b	0.009 a	0.005 a	1.07 a	0.53 a	0.009 a	0.52 a	0.034 a	0.003 a	0.017 b	0.24 a
01 Sep 16	0.34 c	0.031 a	0.013 a	1.32 b	0.0037 b	0.003 b	0.005 b	0.003 a	0.48 b	0.37 b	0.009 a	0.22 b	0.019 b	0.002 b	0.015 b	0.11 b
03 Oct 16	0.70 b	0.030 a	0.014 a	2.48 a	0.0041 a	0.004 a	0.009 a	0.007 a	1.14 a	0.55 a	0.009 a	0.49 a	0.035 a	0.003 a	0.020 a	0.18 a
Distance (Dc)																
2.0 m	0.81 a	0.034 a	0.017 ab	3.09 a	0.0042 a	0.003 a	0.010 a	0.006 ab	1.32 a	0.52 ab	0.009 a	0.51 ab	0.037 a	0.003 a	0.017 a	0.20 ab
5.5 m	0.86 a	0.031 ab	0.021 a	2.81 a	0.0038 a	0.003 a	0.009 a	0.013 a	1.30 a	0.56 a	0.009 a	0.54 a	0.039 a	0.003 a	0.017 a	0.23 a
9.0 m	0.59 b	0.028 b	0.013 b	1.79 b	0.0040 a	0.003 a	0.008 a	0.001 b	0.77 b	0.45 b	0.009 a	0.37 bc	0.025 b	0.003 a	0.018 a	0.15 bc
12.5 m	0.38 c	0.029 ab	0.011 b	1.20 c	0.0042 a	0.003 a	0.005 b	0.004 b	0.51 c	0.41 b	0.009 a	0.27 c	0.020 b	0.002 a	0.016 a	0.10 c
19.5 m	0.47 bc	0.030 ab	0.011 b	1.51 bc	0.0040 a	0.003 a	0.007 ab	0.002 b	0.59 bc	0.47 ab	0.009 a	0.36 bc	0.026 b	0.003 a	0.018 a	0.22 ab
Significance																
Pd	<0.001	0.769	0.151	<0.001	0.009	<0.001	<0.001	0.170	<0.001	<0.001	0.384	<0.001	<0.001	<0.001	<0.001	<0.001
Dc	<0.001	0.011	<0.001	<0.001	0.530	0.498	<0.001	<0.001	<0.001	<0.001	0.075	<0.001	<0.001	0.683	0.513	<0.001
Pd x Dc	<0.001	0.021	<0.001	0.019	0.381	0.079	0.185	0.151	0.001	0.019	0.477	0.066	<0.001	0.039	0.112	0.023

(B) Lawn strip

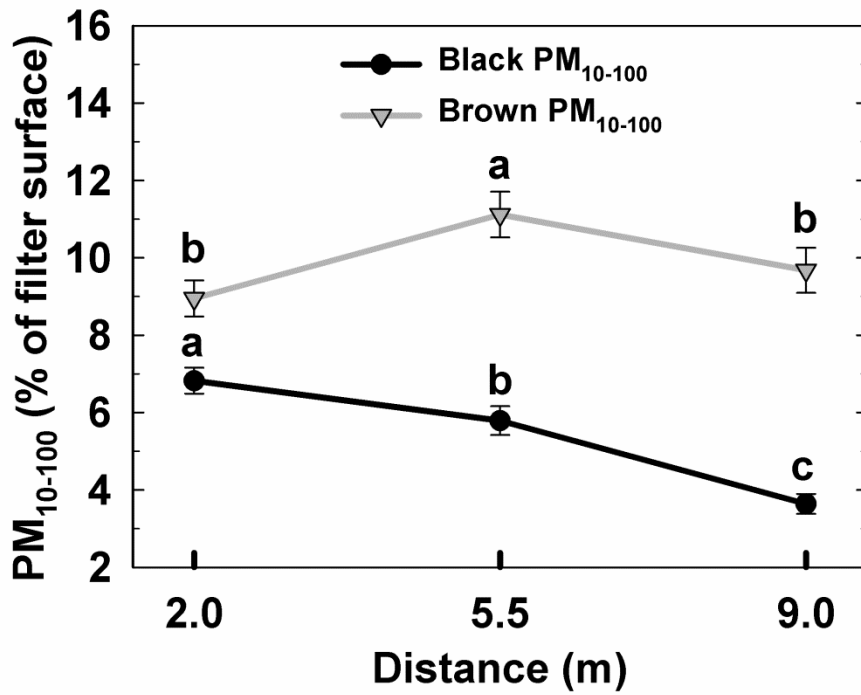
	Al	As	Ba	Ca	Cd	Co	Cr	Cu	Fe	K	Li	Mg	Mn	Mo	Ni	Zn
Period (Pd)																
01 Aug 16	0.587 a	0.032 a	0.015 a	1.78 a	0.0042 ab	0.003 b	0.007 a	0.005 a	0.79 a	0.42 ab	0.009 a	0.34 a	0.025 b	0.003 a	0.014 b	0.16 a
01 Sep 16	0.269 b	0.033 a	0.010 a	0.831 b	0.0031 b	0.002 c	0.004 b	0.001 a	0.37 b	0.33 b	0.009 a	0.14 b	0.014 c	0.002 b	0.011 c	0.06 b
03 Oct 16	0.726 a	0.028 b	0.018 a	2.558 a	0.0042 a	0.004 a	0.007 a	0.005 a	1.22 a	0.51 a	0.009 a	0.52 a	0.036 a	0.002 b	0.019 a	0.14 ab
Distance (Dc)																
2.0 m	0.727 a	0.033 a	0.013 a	2.454 a	0.0036 ab	0.003 a	0.005 b	0.005 a	1.22 a	0.51 a	0.009 ab	0.46 a	0.033 a	0.002 a	0.017 a	0.12 ab
5.5 m	0.773 a	0.033 a	0.021 a	2.412 a	0.0051 a	0.003 a	0.009 a	0.004 a	1.14 ab	0.52 a	0.009 ab	0.48 a	0.031 ab	0.002 a	0.017 a	0.21 a
9.0 m	0.554 ab	0.030 ab	0.019 a	1.701 ab	0.0035 ab	0.003 a	0.007 ab	0.005 a	0.81 abc	0.39 ab	0.009 a	0.33 ab	0.026 ab	0.002 a	0.015 ab	0.09 ab
12.5 m	0.351 ab	0.028 b	0.011 a	1.343 ab	0.0043 ab	0.003 a	0.005 b	0.003 a	0.52 bc	0.39 ab	0.009 ab	0.28 ab	0.019 ab	0.003 a	0.013 ab	0.11 ab
19.5 m	0.233 b	0.031 ab	0.008 a	0.696 b	0.0027 b	0.002 b	0.004 b	0.001 a	0.28 c	0.30 b	0.008 b	0.12 b	0.016 b	0.002 a	0.010 b	0.07 b
Significance																
Pd	0.003	0.001	0.075	0.001	0.035	<0.001	0.006	0.312	0.001	0.001	0.369	0.001	<0.001	0.001	<0.001	0.023
Dc	0.009	0.004	0.050	0.005	0.021	<0.001	0.004	0.816	0.004	0.001	0.048	0.012	0.021	0.039	0.013	0.040
Pd x Dc	0.234	0.001	0.039	0.265	0.11	<0.001	0.006	0.270	0.225	0.060	0.017	0.258	0.131	0.008	0.012	0.075

521 **P-Values* are reported for all factors and for interactions. Different letters indicate significant differences within the same factor and
522 element at $P = 0.05$ using Tukey's test (HSD).

523 3.8 Microscope analysis

524 Percentage values of filter surface occupied by PM₁₀₋₁₀₀ (data not shown) showed very
525 similar trends in terms of species, planting density, sampling period, and distance from the
526 road to those observed for the leaf deposition of PM₁₀₋₁₀₀ (Fig. 2). The area occupied by
527 black PM₁₀₋₁₀₀ (5.41 %) was significantly lower than the area of brown PM₁₀₋₁₀₀ (9.91 %),
528 (Fig. 5). The filters from leaves at 2.0 m from the road were generally characterized by a
529 more marked black coloration (Fig. 6A), while filters from 9.0 m were more brown (Fig.
530 6B). Black PM₁₀₋₁₀₀ showed a constant decrease from the road (2.0 m) to the end of the
531 barrier (9.0 m), while brown PM₁₀₋₁₀₀ had higher values in the middle of the barrier (5.5 m)
532 compared with the other distances (Fig. 5). X-ray microanalysis revealed that black PM<sub>10-
533 100</sub> was mainly composed of C and O with traces of Si (Fig. 6C). In the brown particles, a
534 higher presence of Si, Al, Ca, Fe, Mg and K in addition to C and O was found (Fig. 6D).
535 From the observations of leaf morphology at ESEM, no presence of hairs or trichomes on
536 the upper leaf surface of both species was found (Fig. 7A), while in *V. lucidum*, there were
537 agglomerations of waxes, with a diameter generally lower than 10 μM (Fig. 7E). The lower
538 leaf surface of *P. x fraseri* was smooth (Fig. 7B), while in *V. lucidum*, the presence of
539 trichomes was observed (Fig. 7D).

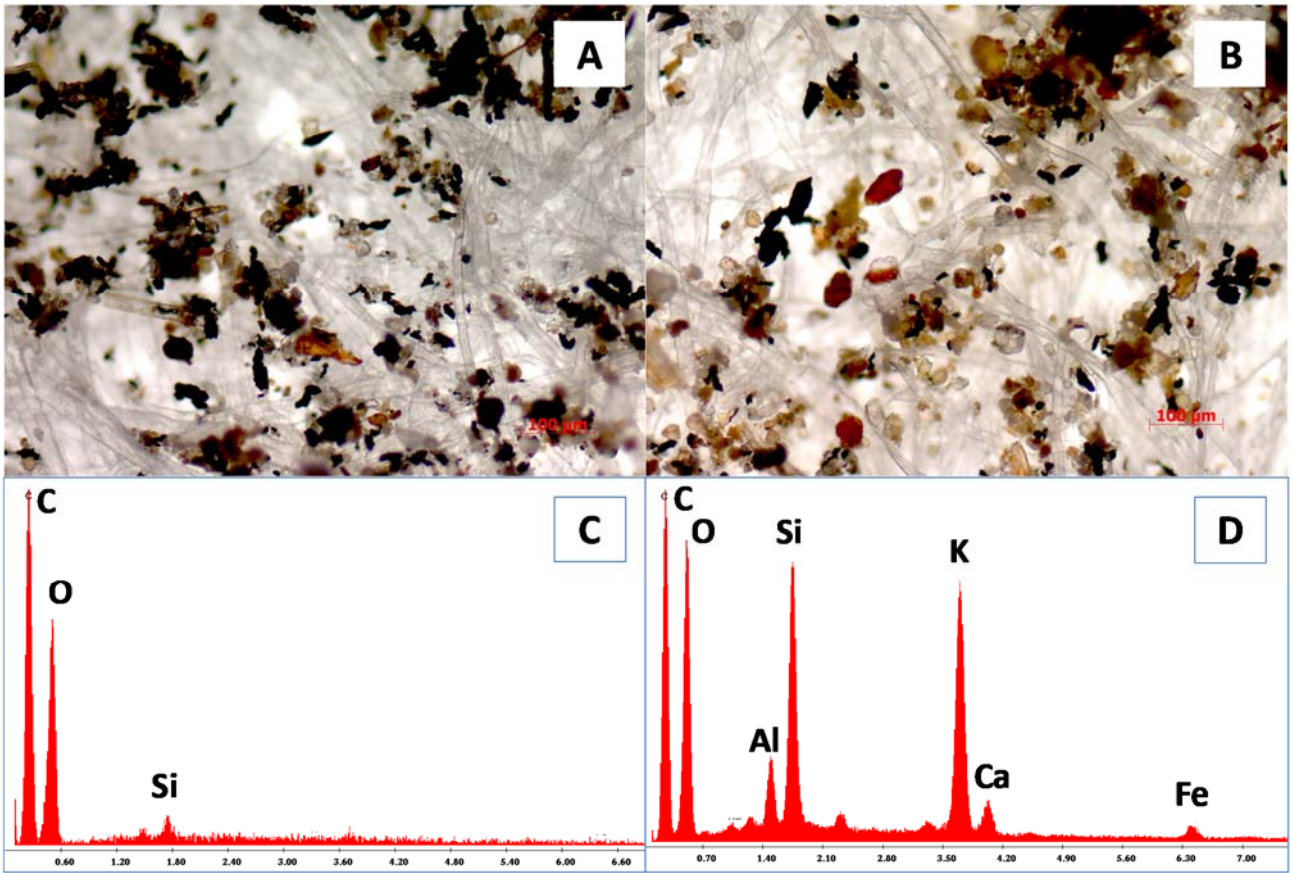
540



541

542 Fig. 5. Percentage of PM₁₀₋₁₀₀ paper filter surface occupied by black and brown particles
 543 derived from leaves washed at different distances from the road. Values are means
 544 (percentage ± SE). Different letters indicate significant differences within the same PM₁₀₋₁₀₀
 545 color at $P= 0.05$ using Tukey's test (HSD).

546



547

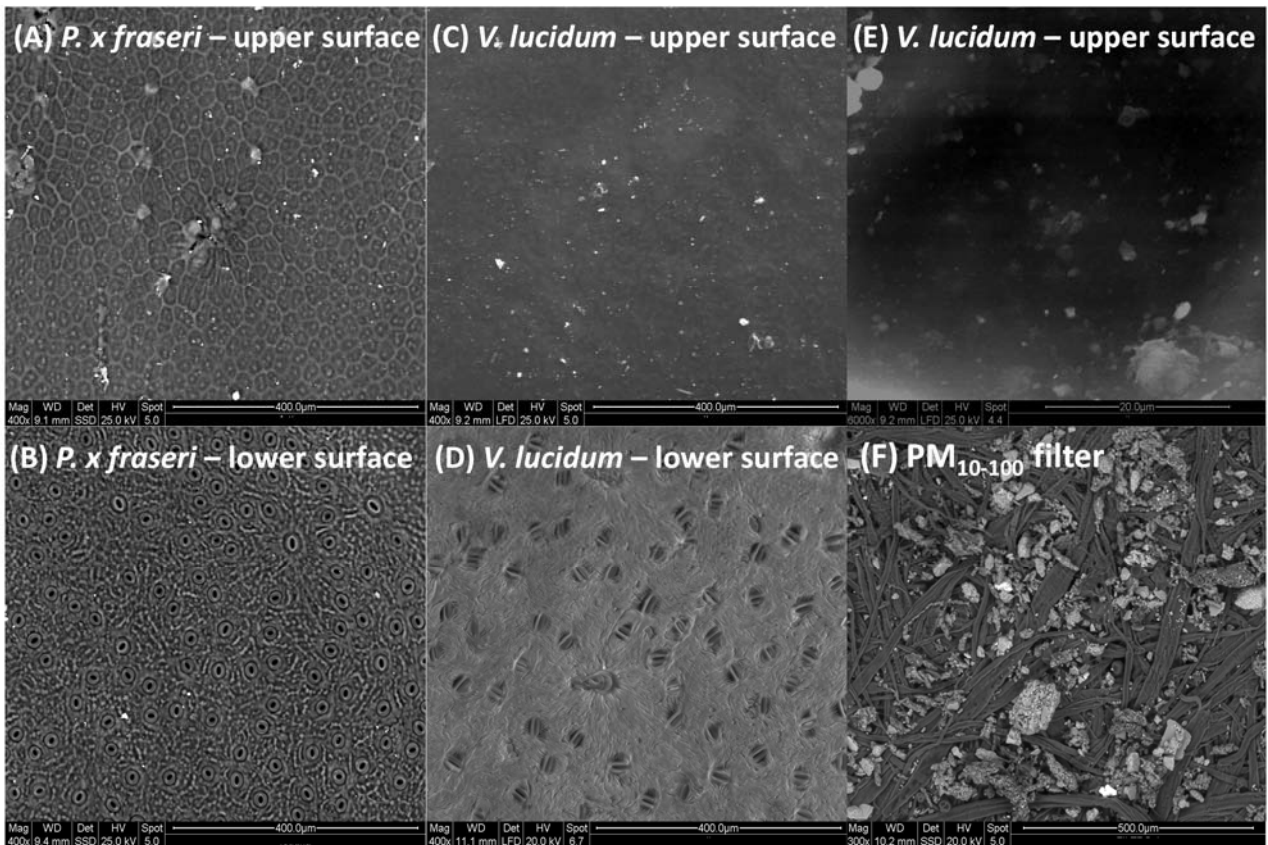
548 Fig. 6. Images at 10x magnification of PM₁₀₋₁₀₀ paper filters (type 91) from (A) leaves at 2.0
 549 m from the road, and from (B) leaves at 9.0 m from the road, carried out with a confocal
 550 microscope. Qualitative element composition in (C) black and (D) brown PM₁₀₋₁₀₀ on type
 551 91 filters carried out using X-ray microanalysis.

552

553

554

555



556

557 Fig. 7. Images taken with an environmental scanning electron microscope (ESEM) at
 558 400x (*P. x fraseri* and *V. lucidum*, A-D), 300x (only upper surface of *V. lucidum*, E) and
 559 6000x (only PM₁₀₋₁₀₀ filter, F) magnification.

560

561 3.9 Relationships between air pollutants and climate parameters

562 Three different groups of air pollutants were identified through correlation analysis (Tab.
 563 B). The first group included air pollutants (PM₁₀₋₁₀₀, Al, Ba, Ca, Co, Cr, Cu, Fe, K, Mg, Ni, V
 564 and Zn) that showed high Pearson's coefficient values with each other ($r = 0.6 - 0.9$) and
 565 poor correlations with the other pollutants ($r \leq 0.3-0.4$). Arsenic, Cd, and Mo formed a
 566 second group with an intermediate degree of correlation with each other ($r = 0.4-0.5$). A
 567 third group consisted of PM_{2.5-10} and PM_{0.2-2.5} which were weakly correlated with each
 568 other at $r = 0.27$ and showed even less correlation with the other variables.

569 Meteorological parameters affected leaf deposition in different ways depending on the
 570 pollutants considered (Tab. B). Increasing air temperatures and increasing wind velocity

571 tended to increase leaf deposition in almost all air pollutants of the previously identified
 572 “first group”, but induced a decrease in As and PM_{2.5-10}. Higher precipitations tended to
 573 decrease almost all the air pollutants in the “first group” and PM_{0.2-2.5} but induced an
 574 increase in As and PM_{2.5-10}.

575 The first three PCA components explained 84.3% of the total variance (Fig. 8). The air
 576 pollutants were differently associated with the first three PCA components obtaining three
 577 different groups (Tab. 5). These groups corresponded well to the three different groups
 578 determined by the correlation analysis (Tab. B).

579 The PCA scores (indicated with circles in Fig. 8), showed how the two species in the third
 580 sampling period (*P. x fraseri* = black full circles; *V. lucidum* = black empty circles) were
 581 differentiated from each other and from the other samples. On the other hand, the samples
 582 from the first and second sampling period (Aug, Sep 16) were not well differentiated from
 583 each other.

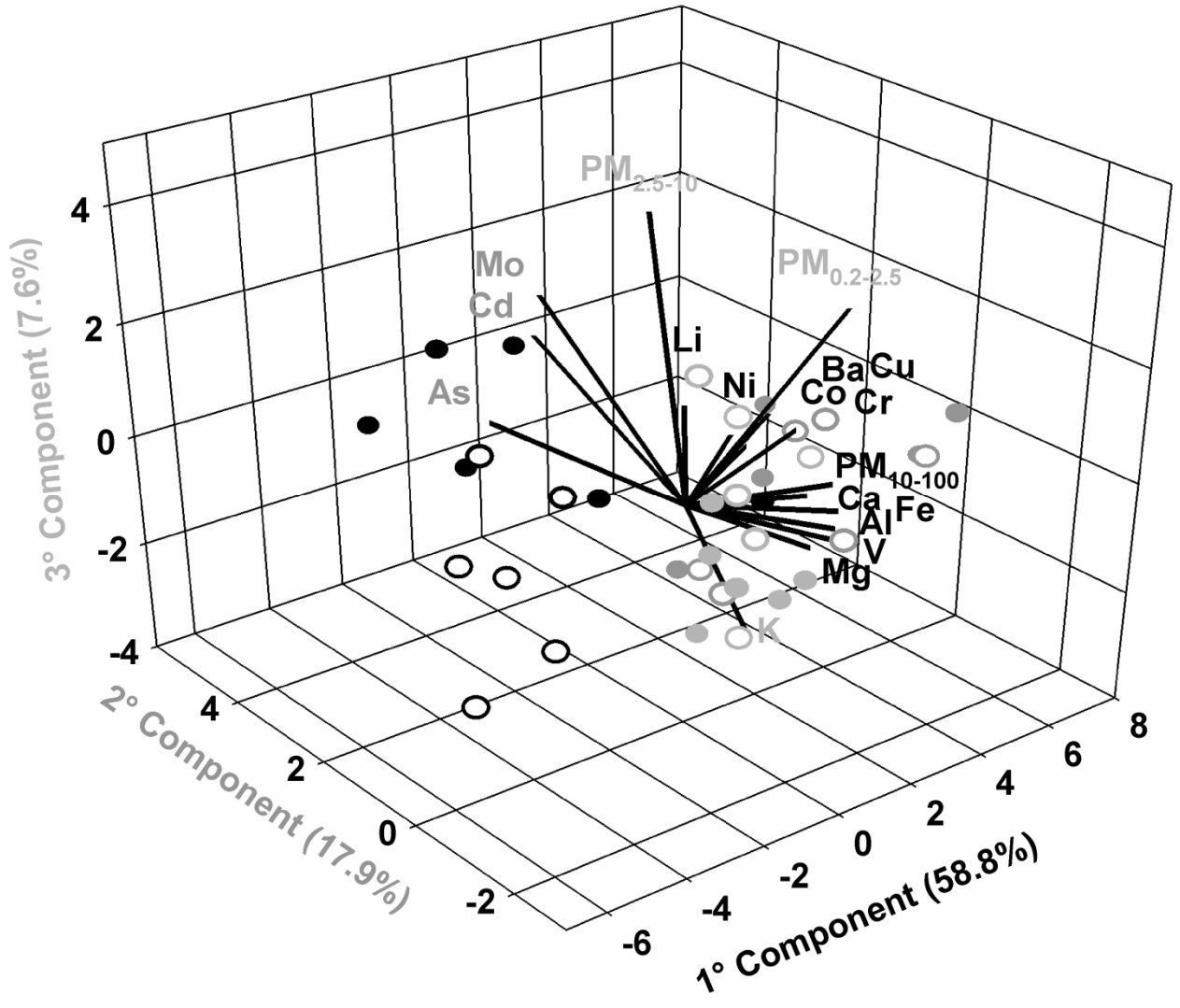
584

585 Tab. 5. Component loadings (i.e. coordinates) of different air pollutants in the first three
 586 components of principal component analysis. The higher component weight in absolute
 587 values of every air pollutant is reported in bold, indicating membership in the respective
 588 component/group.

	Comp. 1- Group 1	Comp. 2 – Group. 2	Comp. 3 – Group. 3
PM ₁₀₋₁₀₀	0.27	-0.15	0.08
PM _{2.5-10}	-0.13	0.01	0.67
PM _{0.2-2.5}	0.03	-0.33	0.48
Al	0.27	-0.16	-0.03
As	-0.01	0.50	-0.05
Ba	0.26	0.00	0.13
Ca	0.28	-0.16	0.04
Cd	0.10	0.46	0.15
K	0.25	0.02	-0.36
Co	0.28	0.06	0.07
Cr	0.29	-0.05	0.16
Cu	0.23	0.06	0.10

Fe	0.30	-0.08	0.03
Li	0.26	0.25	-0.09
Mg	0.29	-0.09	-0.09
Mo	0.11	0.45	0.25
Ni	0.26	0.20	0.11
V	0.29	-0.14	-0.05

589
590



591

592 Fig. 8. 3D-Biplot reporting PCA results carried out on data of PM_x and element leaf
 593 deposition from the entire experiment. The first three components (axes) with the relative
 594 explained variance (%) are reported. Eigenvectors (line-plot) represent the loadings
 595 (coordinates) of different variables (PM_x and elements) on the first three components.
 596 Variables in black, dark grey, and light grey are mainly associated with component 1, 2

597 and 3, respectively. The scatter-plot reports the scores (coordinates) of different samples
598 in relation to the first three components. The full-colored circles represent *P. x fraseri* in the
599 first (light grey), second (dark grey) and third (black) sampling periods. Empty-rimmed
600 circles represent *V. lucidum* in the first (light grey), second (dark grey), and third (black)
601 sampling periods.

602 **4. Discussion**

603 4.1 Experimental site

604 The area surrounding the experimental site showed peri-urban characteristics with a
605 decreasing order in terms of the percentage of occupied land surface between agricultural
606 activities and green areas, buildings and roads and parking, at increasing distances (Tab.
607 2B).

608 The number of vehicles (10,844) passing in front of the experimental field from 7:00 a.m.
609 to 08:00 p.m. was in line with the daily mean of 12,000 previously reported by Mori et al.,
610 (2015a) but was lower compared to other works (Hagler et al., 2012; Brantley et al., 2014;
611 Mori et al., 2015b; Valotto et al., 2015). Despite this, in a previous work (Mori et al., 2015a)
612 we demonstrated that the traffic load was sufficient to produce a detectable deposition of
613 pollutants in the surrounding area.

614

615 4.2 PM_x and element deposition per unit leaf area

616 PM_x deposition on leaves showed similar trends to those observed in previous works
617 carried out with the same methodology but on different species and in different
618 environments (Dzierzanowski et al., 2011; Mori et al., 2015b). Dzierzanowski et al. (2011)
619 reported a mean value of nearly 18 $\mu\text{m cm}^{-2}$ total PM deposited on leaves of eight broad-
620 leaved plant species. Our group (Mori et al., 2015b) found a mean deposition of nearly 16
621 $\mu\text{m cm}^{-2}$ total PM on needles of two coniferous species.

622 The lower PM_{2.5-10} and PM_{0.2-2.5} leaf deposition of *P. x fraseri* (Fig. 2A) compared to *V.*
623 *lucidum* were likely due to the presence of waxes and trichomes, on the upper and lower
624 leaf surfaces respectively, which were observed only in *V. lucidum* (Fig. 7). Waxes and
625 trichomes increase the capacity of leaves to capture particles (Saebo et al., 2012; Popek
626 et al., 2013), especially those lower than 2.5 μm (Tiwary et al., 2005). However, both
627 trichomes and waxes, during the washing-off phase, could have been partially removed

628 from the leaf surface leading to an increase in leaf deposition. Epicuticular waxes can have
629 a considerable weight per unit leaf area (Dzierzanowski et al., 2011). In fact, the size of
630 waxes and trichomes (roughly 10 μm) would explain why the two species only differed in
631 terms of $\text{PM}_{2.5-10}$ and $\text{PM}_{0.2-2.5}$ and not PM_{10-100} (Fig. 2A).

632 Conversely, element deposition per unit leaf area was higher in *P. x fraseri* relative to *V.*
633 *lucidum* (Tab. 3), which indicates that the efficiency of leaves in trapping fine PM differs
634 from elements. This different behavior was also highlighted by correlation: $\text{PM}_{2.5-10}$ and
635 $\text{PM}_{0.2-2.5}$ were generally either not or were weakly correlated with elements, while strong
636 and numerous correlations between PM_{10-100} and elements were found (Tab. B).

637 These results were generally in line with previous works (Li et al., 2003; Araujo and Nel,
638 2009; Mori et al., 2015a), which reported a higher content of metals in the coarser fractions
639 compared to the finer ones, but in contrast with findings reported by Duzgoren-Aydin et al.
640 (2006) and Zannoni et al., (2016). This variability could be related to different
641 environmental factors, i.e., source of emissions, site characteristics, climatic parameters,
642 etc. which have been reported to influence deposition (Adhikari et al 2006; Shah and
643 Shaheen, 2008).

644 The variation in leaf deposition during the different sampling periods confirms their
645 temporary permanence on leaf surface (Nowak et al., 2006). PM_{10-100} and most elements
646 followed a similar trend to each other (Fig. 2C, Tab. 3), which highlighted their close
647 relationship confirmed by correlation analysis (Tab. B) and PCA (Fig. 8, Tab. 5).

648 As reported in the Introduction, climatic parameters have a strong influence on leaf
649 deposition (Beckett et al., 2000; Fowler et al., 2003; Litschke and Kuttler, 2008; Cavanagh
650 et al., 2009). Our findings (Fig. 2C, Tab. 3) regarding the removal action of precipitations
651 and the impact of higher wind speeds, on PM_{10-100} and the deposition of elements on the
652 leaves, were found to be in line with previous studies (Beckett et al., 2000; Nowak et al.,
653 2006). Rain washes off depositions onto the ground, while higher wind speeds tend to

654 increase the deposition velocity, a parameter that is used to describe the phenomena of
655 dry deposition (Fowler et al., 2003; Freer-Smith et al., 2005). In our study, temperature had
656 a contrasting effect on leaf deposition, as previously observed by other authors (Fowler et
657 al., 2003; Litschke and Kuttler, 2008; Cavanagh et al., 2009). PM_{2.5-10}, PM_{0.2-2.5}, As, Cd
658 and Mo showed a different trend over time compared with the remaining air pollutants (Fig.
659 2C, Tab. 3). Smaller particles showed a lower tendency to deposit compared to coarser
660 particles (Fowler et al., 2003). In addition, the deposition of smaller particles is more driven
661 by interception and impaction, while above a 10 µm diameter, gravitational settling prevails
662 (Fowler et al., 2003). A different response to climatic factors may also have contributed to
663 the different trend observed. Przybysz et al. (2014) reported how the finer fraction of PM_x,
664 compared to coarser ones, is less sensitive to the action of rain because of its higher
665 adhesion to leaves. In addition, other works have reported how different air pollutants
666 derived from the same sampling area may show different behaviors depending on the
667 seasonal trend (Adhikari et al 2006; Shah and Shaheen, 2008) and different emission
668 sources (Monaci et al., 2000).

669 In the present work, LAI had a greater effect on leaf deposition than planting density. In *V.*
670 *lucidum*, LAI was similar in terms of high and low planting densities, and no differences in
671 PM_x leaf deposition were found (Fig. 2E, 1F). Conversely, in *P. x fraseri*, the lower LAI
672 observed in the lower planting density induced a significantly lower leaf deposition in PM₁₀₋
673 ₁₀₀ and PM_{2.5-10}.

674 The role of LAI in roadside vegetation barriers in reducing air pollutants was discussed by
675 Hagler et al. (2012). In that case, the unclear effect of vegetation on air pollution was
676 attributed to the low LAI (values around 3) possibly associated with a low rate of
677 interception and impaction of particles on leaf surfaces. In the case of elements, a clearer
678 effect of planting density on leaf deposition was observed with higher values at a higher

679 planting density independently from the species (Tab. 3). Conversely, the effect of LAI on
680 element deposition in the two species was less marked compared to PM_x deposition.
681 It was clear from this and from a previous experiment (Mori et al., 2015a) that the total
682 exposed leaf area affected deposition to a greater extent than leaf morpho-anatomical
683 traits (Tab. A). In fact, barrier transects with a higher total leaf area, had the highest
684 deposition per unit leaf area irrespectively of the species and the planting density (Tab. A).
685 The decrease in leaf deposition of PM_{tot} , PM_{10-100} and most elements at increasing
686 distances from the road (Fig. 2D; Tab. 3) confirmed that vehicular traffic was the main
687 source of pollution in the area. We had previously reached similar conclusions (Mori et al.,
688 2015a), when various multivariate statistical methods were used to identify the possible
689 source of leaf deposition of elements in the same experimental area. The fact that only the
690 coarser fractions of PM_x decreased significantly at increasing distances may be linked to
691 the larger diameters associated with a higher tendency to deposition (Fowler et al., 2003)
692 compared with $PM_{2.5-10}$, and $PM_{0.2-2.5}$, which instead had a higher dispersion capacity.
693 In a previous work (Mori et al., 2015b), we found a significant reduction in large PM and 14
694 elements on needles of *Picea sitchensis* between a distance of 5 and 25 m from the road.
695 In contrast, Peachey et al. (2009) did not find significant differences in soluble
696 concentrations of eight metals in leaves of four tree species at 0, 2, 4, 6 and 12 m from the
697 road. The higher leaf deposition of PM_x and most elements at 1.5 m from the ground
698 compared with a 3.0 m height (Fig. 2; Tab. 3) confirmed the contribution of traffic to the
699 presence of air pollutants. In fact, as reported by Etyemezian et al. (2004), when
700 vegetation is within a distance of 20 m from the road verge, the impact zone on plants of
701 the dust plume from traffic is concentrated in the first two meters from the ground.

702

703 4.3 PM_x and elements in the experimental site

704 The deposition of PM_x in the experimental site during the different sampling periods
705 partially differed from the element deposition (Tab. 4; Fig. 3). From August to September
706 both PM_x and elements generally decreased, likely due to lower traffic emissions during
707 the summer holiday. From September to October on the other hand, a more
708 heterogeneous response was observed with increasing elements and decreasing PM_x
709 deposition. The latter were in agreement with the PM_x leaf deposition (Fig. 2). A similar
710 variability was observed in previous works and was related to different responses to
711 environmental factors (Adhikari et al 2006; Nowak et al., 2006; Shah and Shaheen, 2008)
712 as also observed in the present work (Fig. 8 and Tab. B). In fact, although elements are
713 commonly associated with PM_x (Valotto et al., 2015), they have been found to show a
714 different trend since they are also directly released from tires, brakes or other parts of
715 vehicles (Adhikari et al 2006; Nowak et al., 2006; Shah and Shaheen, 2008; Zannoni et al.,
716 2016). Considering the strong influence of particle diameter on deposition dynamics
717 (Fowler et al., 2003), it is possible to understand how the deposition dynamics of elements
718 can change depending on their association with PM.

719 The deposition in the experimental area (passive samplers) showed different dynamics
720 compared with the leaf deposition. This may be the consequence of several factors: i)
721 leaves were exposed to traffic emissions throughout the entire experiment, while PTFE
722 membranes were renewed at each sampling; ii) the action of climatic factors, especially
723 rain, on PTFE membranes was partially limited by the structure of the passive samplers;
724 iii) the surface of PTFE membranes and leaves have very different physical
725 characteristics, height from the ground and angle of exposure.

726 The presence of the vegetation barrier induced a modification in the deposition of air
727 pollutants in the experimental site (Fig. 3C, Fig. 3D, Fig. 4, Tab. 4). In general, vegetation
728 barriers and high vegetation modify the direction and reduce the velocity of the impacting
729 air fluxes (Tiway et al., 2005). This thus promotes the deposition of particles greater than

730 0.1 μm through interception, impaction and gravitational settling (Fowler et al., 2003;
731 Freer-Smith et al., 2005). The velocity reduction of the impacting air fluxes can occur
732 within the barrier and in the first meters downwind of the vegetation because of partial air
733 stagnation (Tiwary et al., 2005). In the stagnation area, there may be a higher air pollution
734 concentration and a higher gravitational deposition may occur, especially for coarser
735 particles (Fowler et al., 2003). In line with this, Hagler et al. (2012) reported that vegetation
736 “may reduce air flow leading to increased pollutant concentrations due to the more
737 stagnant conditions within and behind the trees”. This explains why the PM_{10-100} and $\text{PM}_{2.5-10}$
738 deposition tended to be higher in the middle and just behind the barrier (5.5 m and 9.0
739 from the road) compared to the other sampling distances. Conversely, in the lawn strip, the
740 absence of obstacles led to an even drift of PM_x from the road.

741 The more marked decrease of elements at increasing distances from the road and the
742 higher total deposition of 8 out of 21 elements observed in the barrier strip compared with
743 the lawn strip (Tab. 4; Fig. 4), could be directly related to the capacity of the vegetation to
744 limit the drift of air pollutants from the road to the area close to the barrier. In fact,
745 deposition increases at higher air concentrations of air pollutants (Fowler et al., 2003).
746 Previous works have used both field measurements and models to investigate roadside
747 vegetation barriers with comparable dimensions to those of the vegetation barrier of the
748 present work (Hagler et al., 2012; Brantley et al., 2014; Morakinyo and Lam, 2016) with
749 contrasting results on the effects on air pollution concentration.

750 Considering the diversity between air pollution concentrations and air pollutant deposition,
751 the percentage reduction of the concentration of air pollution behind the roadside
752 vegetation barriers (Tiwary et al., 2008; Chen et al., 2015; Lin et al., 2016) was in
753 agreement with findings in the present work between the barrier and lawn strips (Fig. 3).

754 The lack of significant differences in the deposition of PM_x and elements between the lawn

755 and the barrier strip in front of the road (2 m) suggests the uniformity of exposure of the
756 entire experimental site to the traffic-deriving pollutant fluxes.

757

758 4.4 Microscope analysis

759 The similarities between the results of PM₁₀₋₁₀₀ leaf deposition (Fig. 2) and the percentage
760 of filter paper surface occupied by of PM₁₀₋₁₀₀ (data not shown) confirm the reliability of
761 both methods for investigating leaf deposition. The use of image analysis differentiated
762 between on-leaf PM₁₀₋₁₀₀ with different colorations, thus highlighting the different deposition
763 at different distances from the road between black and brown particles (Fig. 5). To our
764 knowledge, no previous studies have used image analysis with the same aim. The
765 association between image analysis and X-ray microanalysis (Fig. 6) enabled us to
766 determine the element composition of the black and brown particles separately. Although
767 X-ray microanalysis has already been used to detect the element composition of particles
768 (Sgrigna et al., 2015), selectively analyzing PM on the basis of their color may represent a
769 novelty. The different presence at different distances from the road (Fig. 5) and the
770 different element composition between black and brown PM₁₀₋₁₀₀, suggest a different
771 origin. In particular black particles, which showed a progressive decrease from the road
772 and an almost complete composition in C and O, are probably black carbon which is a
773 typical component of PM derived from traffic (Ferrero et al., 2014). Brown particles on the
774 other hand may be due to the contribution of soil, considering both the lack of a clear
775 reduction far from the road and the presence of several typical elements from soil such as
776 Si, Al, K etc., (Zhao et al., 2006).

777

778 **Conclusions**

779 Different species showed a different deposition per unit leaf area with higher PM_{2.5-10} and
780 PM_{0.2-2.5} in *V. lucidum* and a higher presence of elements in *P. x fraseri*, indicating a

781 different capacity to remove different types of air pollutants. A higher LAI induced a higher
782 deposition per unit leaf area, while a higher plant density was not a determining factor.
783 The barrier strip at 19.5 m from the road showed a 31 % and 32 % lower deposition for
784 PM_{tot} and PM_{10-100} respectively, compared with the lawn strip. In addition deposition in the
785 barrier strip at different distances showed a bell-shaped trend, while in the lawn strip no
786 significant difference was found. The barrier strip induced a higher element deposition
787 compared to the lawn strip with a more marked decreasing trend at increasing distances
788 from the road.

789

790 **Funding**

791 This research did not receive any specific grant from funding agencies in the public,
792 commercial, or not-for-profit sectors.

793

794 **References**

- 795 Abhijith, K.V., Kumar, P., Gallagher, J., McNabola, A., Baldauf, R., Pilla, F., Broderick, B.,
796 Di Sabatino, S., Pulvirenti, B., 2017. Air pollution abatement performances of green
797 infrastructure in open road and built-up street canyon environments - A review.
798 Atmospheric Environment 162, 71-86.
799 <https://doi.org/10.1016/j.atmosenv.2017.05.014>
- 800 Adhikari, A., Reponen, T., Grinshpun, S.A., Martuzevicius, D., LeMasters G., 2006.
801 Correlation of ambient inhalable bioaerosols with particulate matter and ozone: A
802 two-year study. Environmental Pollution 140, 16-28.
803 <https://doi.org/10.1016/j.envpol.2005.07.004>
- 804 Al-Dabbous, A.N., Kumar, P., 2014. The influence of roadside vegetation barriers on
805 airborne nanoparticles and pedestrians exposure under varying wind conditions.

806 Atmospheric environment 90, 113-124.
807 <https://doi.org/10.1016/j.atmosenv.2014.03.040>

808 Aničić, M., Spasic, T., Tomašević, M., Rajšić, S., Tasic, M., 2011. Trace element
809 accumulation and temporal trends in leaves of urban deciduous trees (*Aesculus*
810 *hippocastanum* and *Tilia* spp.). *Ecological Indicators* 11, 824–830.
811 <https://doi.org/10.1016/j.ecolind.2010.10.009>

812 Araujo, J.A., Nel, A.E., 2009. Particulate matter and atherosclerosis: role of particle size,
813 composition and oxidative stress. *Particle Fibre Toxicology* 6, 24.
814 <https://doi.org/10.1186/1743-8977-6-24>.

815 Baldauf, R., 2017. Roadside vegetation design characteristics that can improve local,
816 near-road air quality. *Transportation Research Part D: Transport and Environment*,
817 52, 354-361. <http://dx.doi.org/10.1016/j.trd.2017.03.013>

818 Bealey, W.J., McDonald, A.G., Nemitz, E., Donovan, R., Dragosits, U., Duffy, T.R., Fowler,
819 D., 2007. Estimating the reduction of urban PM 10 concentrations by trees within an
820 environmental information system for planners. *Journal of Environmental*
821 *Management*. 85, 44–58. <https://doi.org/10.1016/j.jenvman.2006.07.007>

822 Beckett, K.P., Freer-Smith, P.H., Taylor, G., 2000. Particulate pollution capture by urban
823 trees: effect of species and wind speed. *Global Change Biology* 6, 995–1003.
824 <https://doi.org/10.1046/j.1365-2486.2000.00376.x>

825 Bell, M.L., Morgenstern, R.D., Harrington, W., 2011. Quantifying the human health benefits
826 of air pollution policies: review of recent studies and new directions in accountability.
827 *Environmental Science & Policy* 14, 357–368.
828 <https://doi.org/10.1016/j.envsci.2011.02.006>

829 Brantley, H.L., Hagler, G.S.W., Deshmukh, P.J., Baldauf, R.W., 2014. Field assessment of
830 the effects of roadside vegetation on near-road black carbon and particulate matter.

831 Science of the Total Environment 468–469, 120–129.
832 <http://dx.doi.org/10.1016/j.scitotenv.2013.08.001>

833 Buccolieri, R., Gromke, C., Di Sabatino, S., Ruck, B., 2009. Aerodynamic effects of trees
834 on pollutant concentration in street canyons. *Science of the Total Environment* 407,
835 5247-5256. <https://doi.org/10.1016/j.scitotenv.2009.06.016>

836 Catoni, R., Gratani L., 2014. Variations in leaf respiration and photosynthesis ratio in
837 response to air temperature and water availability among Mediterranean evergreen
838 species. *Journal of Arid Environments* 102, 82-88.
839 <https://doi.org/10.1016/j.jaridenv.2013.11.013>

840 Cavanagh, J.E., Zawar-Reza, P., Wilson, G., 2009. Spatial attenuation of ambient
841 particulate matter air pollution within an urbanised native forest patch. *Urban Forestry
842 & Urban Greening* 8, 21–30. <https://doi.org/10.1016/j.ufug.2008.10.002>

843 Chen, X., Pei T., Zhou, Z., Teng, M., He, L., Luo, M., Liu, X., 2015. Efficiency differences
844 of roadside greenbelts with three configurations in removing coarse particles (PM10):
845 A street scale investigation in Wuhan, China. *Urban Forestry & Urban Greening* 14,
846 354–360. <https://doi.org/10.1016/j.ufug.2015.02.013>

847 Duzgoren-Aydin, N.S., Wong, C.S.C., Aydin, A., Song, Z., You, M., Li, X.D., 2006. Heavy
848 metal contamination and distribution in the urban environment of Guangzhou, China.
849 *Environmental Geochemistry and Health* 28, 375–391. [https://doi.org
850 /10.1007/s10653-005-9036-7](https://doi.org/10.1007/s10653-005-9036-7)

851 Dzierzanowski, K., Popek, R., Gawronska, H., Sæbø, A., Gawronski, S.W., 2011.
852 Deposition of particulate matter of different size fractions on leaf surfaces and in
853 waxes of urban forest species. *International Journal of Phytoremediation* 13, 1037–
854 1046. <https://doi.org/10.1080/15226514.2011.552929>

855 EEA, 2017. Air quality in Europe report 13, 8.

856 Etyemezian, V., Gillies, J., Kuhns, H., Nikolic, D., Watson, J., Veranth, J., Labban, R.,
857 Seshadri, G., Gillett, D., 2003. Field testing and evaluation of dust deposition and
858 removal mechanisms: Final report; report prepared for WESTAR council, Lake
859 Oswego, OR, by DRI: Las Vegas, NV, USA.

860 Etyemezian, V., Ahonen, S., Nikolic, D., Gillies, J., Kuhns, H., Gillette, D., Veranth, J.,
861 2004. Deposition and removal of fugitive dust in the arid Southwestern United States:
862 measurements and model results. *Journal of the Air & Waste Management*
863 *Association* 54, 1099-1111. <https://doi.org/10.1080/10473289.2004.10470977>

864 Ferrero, L., Castelli M., Ferrini, B.S., Moscatelli, M., Perrone, M.G., Sangiorgi, G.,
865 D'Angelo, L., Rovelli, G., Moroni, B., Scardazza, F., Mocnik, G., Bolzacchini, E.,
866 Petitta, M., Cappelletti, D., 2014. Impact of black carbon aerosol over Italian basin
867 valleys: high-resolution measurements along vertical profiles, radiative forcing and
868 heating rate. *Atmospheric Chemistry & Physics* 14, 9641–9664.
869 <https://doi.org/10.5194/acp-14-9641-2014>

870 Fowler, D., Skiba, U., Nemitz, E., Choubedar, F., Branford, D., Donovan, R., Rowland, P.,
871 2003. Measuring aerosol and heavy element deposition on urban woodland and
872 grass using inventories of ²¹⁰Pb and element concentrations in soil. *Water Air & Soil*
873 *Pollution* 4, 483–499. <https://doi.org/10.1023/B:WAFO.0000028373.02470.ba>

874 Freer-Smith, P.H., Beckett, K.P., Taylor, G., 2005. Deposition velocities to *Sorbusaria*,
875 *Acer campestre*, *Populus deltoides* × *trichocarpa* 'Beaupré', *Pinus nigra* and *X*
876 *Cupressocyparis leylandii* for coarse, fine and ultra-fine particles in the urban
877 environment. *Environmental Pollution* 133, 157–167. [https://doi.org](https://doi.org/10.1016/j.envpol.2004.03.031)
878 [10.1016/j.envpol.2004.03.031](https://doi.org/10.1016/j.envpol.2004.03.031)

879 Hagler, G.S.W., Lin, M.Y., Khlystov, A., Baldauf, R.W., Isakov, V., Faircloth, J., Jackson,
880 L.E., 2012. Field investigation of roadside vegetative and structural barrier impact on

881 near-road ultrafine particle concentrations under a variety of wind conditions. *Science*
882 *of the Total Environment*. 419, 7-15. <https://doi.org/10.1016/j.scitotenv.2011.12.002>.

883 Irga, P.J., Burchett, M.D., Torpy, F.R., 2015. Does urban forestry have a quantitative effect
884 on ambient air quality in an urban environment? *Atmospheric Environment* 120: 173-
885 181. <https://doi.org/10.1016/j.atmosenv.2015.08.050>

886 Janhäll, S., 2015. Review on urban vegetation and particle air pollution deposition and
887 dispersion. *Atmospheric Environment* 105, 130-137.
888 <https://doi.org/10.1016/j.atmosenv.2015.01.052>

889 Jeanjean, A.P.R., Buccolieri, R., Eddy, J., Monks, P. S., Leigh R.J. 2017. Air quality
890 affected by trees in real street canyons: The case of Marylebone neighbourhood in
891 central London. *Urban Forestry & Urban Greening* 22, 41–53.
892 <https://doi.org/10.1016/j.ufug.2017.01.009>

893 Li, N., Hao, M., Phalen, R.F., Hinds, W.C., Nel, A.E., 2003. Particulate air pollutants and
894 asthma: a paradigm for the role of oxidative stress in PM-induced adverse health
895 effects. *Clinical Immunology* 109, 250–265. <https://doi.org/10.1016/j.clim.2003.08.006>

896 Lin, M.Y., Hagler, G., Baldauf, R., Isakov, V., Lin, H.Y., Khlystov, A., 2016. The effects of
897 vegetation barriers on near-road ultrafine particle number and carbon monoxide
898 concentrations. *Science of the Total Environment* 553, 372–379.
899 <https://doi.org/10.1016/j.scitotenv.2016.02.035>

900 Litschke, T., Kuttler, W., 2008. On the reduction of urban particle concentration by
901 vegetation; a review. *Meteorologische Zeitschrift* 17, 229-240.

902 Lorenzini, G., Grassi, C., Nali, C., Petiti, A., Loppi, S., Tognotti, L., 2006. Leaves of
903 *Pittosporum tobira* as indicators of airborne trace element and PM10 distribution in
904 central Italy. *Atmospheric Environment* 40, 4025-4036.
905 <https://doi.org/10.1016/j.atmosenv.2006.03.032>

906 Monaci, F., Moni, F., Lanciotti, E., Grechi, D., Bargagli, R., 2000. Biomonitoring of airborne
907 elements in urban environments: new tracers of vehicle emission, in place of lead.
908 *Environmental Pollution* 107, 321–327. [https://doi.org/10.1016/S0269-](https://doi.org/10.1016/S0269-7491(99)00175-X)
909 [7491\(99\)00175-X](https://doi.org/10.1016/S0269-7491(99)00175-X)

910 Morakinyo, T.E. & Lam Y.F., 2016. Simulation study of dispersion and removal of
911 particulate matter from traffic by road-side vegetation barrier. *Environmental Science*
912 *& Pollution Research* 23, 6709–6722. <https://doi.org/10.1007/s11356-015-5839-y>

913 Mori, J., Sæbø, A., Hans Hanslin, H.M., Teani, A., Ferrini, F., Fini, A., Burchi, G., 2015a.
914 Deposition of traffic related air pollutants on leaves of six evergreen shrub species
915 during Mediterranean summer season. *Urban Forestry & Urban Greening* 14, 264–
916 273. <https://doi.org/10.1016/j.ufug.2015.02.008>

917 Mori, J., Hans Hanslin, H.M., Burchi, G., Sæbø, A., 2015b. Particulate matter and element
918 accumulation on coniferous trees at different distances from a highway. *Urban*
919 *Forestry & Urban Greening* 14, 170–177. <https://doi.org/10.1016/j.ufug.2014.09.005>

920 Mori, J., Fini A., Burchi, G., Ferrini, F., 2016. Carbon uptake and air pollution mitigation of
921 different Evergreen shrub species. *Arboriculture and Urban Forestry*, 42(5), 329- 345.

922 Neft, I., Scungio, M., Culver, N., Singh, S., 2016. Simulations of aerosol filtration by
923 vegetation: validation of existing models with available lab data and application to
924 near-roadway scenario. *Aerosol Sci. Technol.* 50 (9), 937–946.
925 <https://doi.org/10.1080/02786826.2016.1206653>

926 Nowak, D.J., Crane, D.E., Stevens, J.C., 2006. Air pollution removal by urban trees and
927 shrubs in the United States. *Urban Forestry & Urban Greening* 4, 115–123.
928 <https://doi.org/10.1016/j.ufug.2006.01.007>

929 Nowak, D.J., Hirabayashi, S., Bodine, A., Hoehn, R., 2013. Modeled PM_{2.5} removal by
930 trees in ten U.S. cities and associated health effects. *Environmental Pollution* 178,
931 395-402. <https://doi.org/10.1016/j.envpol.2013.03.050>

932 Peachey, C.J., Sinnett, D., Wilkinson, M., Morgan, G.W., Freer-Smith, P.H., Hutchings,
933 T.R., 2009. Deposition and solubility of airborne elements to four plant species grown
934 at varying distances from two heavily trafficked roads in London. *Environmental*
935 *Geochemistry and Health* 31, 315–325. <https://doi.org/10.1016/j.envpol.2009.03.032>

936 Petroff, A., Mailliat, A., Amielh, M., Anselmet, F., 2008. Aerosol dry deposition on
937 vegetative canopies. Part I: review of present knowledge. *Atmospheric Environment*
938 42, 3625-3653. <https://doi.org/10.1016/j.atmosenv.2007.09.043>

939 Pikridas, M., Tasoglou, A., Florou, K., Pandis, S.N., 2013. Characterization of the origin of
940 fine particulate matter in a medium size urban area in the Mediterranean.
941 *Atmospheric Environment* 80, 264–274.
942 <https://doi.org/10.1016/j.atmosenv.2013.07.070>

943 Popek, R., Gawronska, H., Wrochna, M., Gawroński, S.W., Sæbø, A., 2013. Particulate
944 matter of foliage of 13 woody species: deposition on surfaces and phytostabilisation
945 in waxes – a 3 –year study. *International Journal of Phytoremediation* 15 (3), 245 –
946 256. <http://dx.doi.org/10.1080/15226514.2012.694498>

947 Popek, R., Łukowski, A., Bates, C., Oleksyn, J., 2017. Particulate matter, heavy metals
948 and polycyclic aromatic hydrocarbons accumulation on the leaves of *Tilia cordata*
949 Mill. in five Polish cities with different level of air pollution. *Inter. Journal of*
950 *Phytoremediation* 19 (12), 1134-1141.
951 <http://doi.org/10.1080/15226514.2017.1328394>

952 Przybysz, A., Sæbø, A., Hanslin, H., Gawroński, S., 2014. Accumulation of particulate
953 matter and trace elements on vegetation as affected by pollution level, rainfall and
954 the passage of time. *Science of the Total Environment* 481, 360-369.
955 <http://doi.org/10.1016/j.scitotenv.2014.02.072>

956 Pugh, T.A.M., A.R. MacKenzie, J.D. Whyatt, and C.N. Hewitt. 2012. Effectiveness of green
957 infrastructure for improvement of air quality in urban street canyons. *Environmental*
958 *Science and Technology* 46(14), 7692–7699. DOI: 10.1021/es300826w

959 Sæbø, A., Popek, R., Nawrot, B., Hanslin, H.M., Gawronska, H., Gawronski, S.W., 2012.
960 Plant species differences in particulate matter accumulation on leaf surfaces. *Science*
961 *of the Total Environment* 427–428, 347–354.
962 <https://doi.org/10.1016/j.scitotenv.2012.03.084>

963 Sawidis, T., Breuste, J., Mitrovic, M., Pavlovic, P., Tsigaridas, K., 2011. Trees as
964 bioindicator of heavy element pollution in three European cities. *Environmental*
965 *Pollution* 159, 3560–3570. <https://doi.org/10.1016/j.envpol.2011.08.008>

966 Sgrigna G., Baldacchini C., Esposito R., Calandrelli R., Tiwary A., Calfapietra C., 2015.
967 Characterization of leaf-level particulate matter for an industrial city using electron
968 microscopy and Xray microanalysis. *Science of the Total Environment* 548–549, 91–
969 99. <https://doi.org/10.1016/j.scitotenv.2016.01.057>

970 Shah, M.H. and Shaheen, N., 2008. Annual and seasonal variations of trace metals in
971 atmospheric suspended particulate matter in Islamabad, Pakistan. *Water Air & Soil*
972 *Pollution* 190, 13–25. <https://doi.org/10.1007/s11270-007-9575-x>

973 Skrbic, B., Milovac, S., Matavulj, M., 2012. Multielement profiles of soil, road dust, tree
974 bark and wood-rotten fungi collected at various distances from high- frequency road
975 in urban area. *Ecological Indicators* 13, 168–177.
976 <https://doi.org/10.1016/j.ecolind.2011.05.023>

977 Tiwary, A., Morvan, H.P., Colls, J.J., 2005. Modelling the size-dependent collection
978 efficiency of hedgerows for ambient aerosols. *Journal of Aerosol Science* 37, 990–
979 1015. <https://doi.org/10.1016/j.jaerosci.2005.07.004>

980 Tiwary, A., Reff, A., Colls, J.J., 2008. Collection of ambient particulate matter by porous
981 vegetation barriers: Sampling and characterization methods. *Journal of Aerosol*
982 *Science* 39, 40–47. <https://doi.org/10.1016/j.jaerosci.2007.09.011>

983 Thurston, G.D., 2008. Outdoor air pollution: sources, atmospheric transport, and human
984 health effects. In: Kris, H. (Ed.), *International Encyclopedia of Public Health*.
985 Academic Press, Oxford, 700-712. [https://doi.org/10.1016/B978-012373960-](https://doi.org/10.1016/B978-012373960-5.00275-6)
986 [5.00275-6](https://doi.org/10.1016/B978-012373960-5.00275-6)

987 United Nations, 2014. *World urbanization prospects – 2014 revision*.

988 Valotto, G., Rampazzo, G., Visin, F., Gonella, F., Cattaruzza, E., Glisenti, A., Formenton,
989 G., Tieppo, P., 2015. Environmental and traffic-related parameters affecting road dust
990 composition: a multi-technique approach applied to Venice area (Italy). *Atmospheric*
991 *Environment* 122, 596-608. <https://doi.org/10.1016/j.atmosenv.2015.10.006>

992 World Health Organisation (WHO), 2014. *Burden of Disease from Ambient Air Pollution for*
993 *2012*. The World Health Organisation, Geneva Switzerland.

994 Zannoni, D., Valotto, G., Visin, F., Rampazzo, G., 2016. Sources and distribution of tracer
995 elements in road dust: The Venice mainland case of study. *Journal of Geochemical*
996 *Exploration* 166, 64–72. <https://doi.org/10.1016/j.gexplo.2016.04.007>

997 Zhao, P., Feng, Y., Zhu, T., Wu, J., 2006. Characterizations of resuspended dust in
998 sixcities of North China. *Atmospheric Environment* 40, 5807–5814.
999 <https://doi.org/10.1016/j.atmosenv.2006.05.026>